Title: Legacy effects of precipitation and land use impact maize growth and microbiome assembly under drought stress

Running Title: Maize Drought Microbiome

Authors

Joel F. Swift[1,2*], Matthew R. Kolp[1,2,4], Amanda Carmichael[1,4], Natalie E. Ford[1], Paige M. Hansen[2,4], Benjamin A. Sikes[1,2], Manuel Kleiner[3], Maggie R. Wagner[1,2*]

Affiliations

[1] Department of Ecology and Evolutionary Biology, University of Kansas, Lawrence, KS 66045

[2] Kansas Biological Survey & Center for Ecological Research, University of Kansas, Lawrence, KS 66045

[3] Department of Plant and Microbial Biology, North Carolina State University, Raleigh, NC, 27695

[4] Current Address: Center for Animal and Human Health in Appalachia, College of Veterinary Medicine, Lincoln Memorial University, Harrogate, TN 37752 (M.R.K.); Department of Conservation and Research, Southeastern Center for Conservation, Atlanta Botanical Garden, Atlanta, GA, 30309 (A.C.); Department of Soil and Crop Science, Colorado State University, Fort Collins, CO 80521 (P.M.H.)

*Correspondence: joel.swift@ku.edu and maggie.r.wagner@ku.edu

Abstract

As the climate changes, plants and their associated microbiomes face greater water limitation and increased frequency of drought. Historical precipitation patterns can leave a legacy effect on soil and root-associated microbiomes, but the impact of this conditioning on future drought performance is poorly understood. Moreover, agricultural practices, like irrigation, tillage, and fertilization, may disrupt precipitation legacies in natural systems. Precipitation gradients provide a means to assess these legacy effects. We collected soil microbiomes across a Kansas precipitation gradient from two agricultural fields and four native prairies. Seedlings of two *Zea mays* genotypes were inoculated with each soil microbiome in a factorial drought experiment. Drought caused

plants to accumulate shoot mass more slowly and achieve greater root/shoot mass ratios. Drought restructured the bacterial root-associated microbiome, via depletion of Pseudomonadota and enrichment of Actinomycetota, whereas the fungal microbiome was largely unaffected. A historical precipitation legacy effect on prairie soil microbiomes interacted with plants during drought treatment. Prairie soil inocula from historically wetter locations increased shoot biomass under drought more than historically drier prairie soils. Agriculturally derived soil microbiomes tended to reduce biomass accumulation rates, with genotype-specific impacts. We demonstrate links between soil microbiome legacy effects and plant performance under drought, suggesting that future drying climates may condition soils to negatively impact plant performance.

Introduction

Increasing drought frequency due to global climate change will impact both soil and plant-associated microbiomes (Chiang *et al.* 2021; Balting *et al.* 2021). Drought directly limits microbial growth, mobility, and access to resources, but also alters plant host traits (e.g., root physiology, morphology, and exudate composition) that comprise the habitat available to root-associated microorganisms (Naylor and Coleman-Derr 2018). Historical precipitation patterns and drought can leave lasting impacts, or legacy effects, on soil and root-associated microbiomes. Naturally-occurring precipitation gradients—which shape the biogeography of both plants (Field *et al.* 2009; Korell *et al.* 2021) and soil microorganisms (Bachar *et al.* 2010; Hawkes *et al.* 2011)—provide opportunities to study legacy effects of precipitation on plant-microbe interactions. Historical patterns of water availability across gradients constrain the functional potential of soil microbiomes (Hawkes and Keitt 2015; Averill *et al.* 2016; Canarini *et al.* 2021); however, the implications for host plants, including agricultural, are not well understood.

Plants recruit root microbes primarily from the soil (Zarraonaindia *et al.* 2015), and we would expect drought-induced changes in the soil microbiome to be reflected in root-associated microbiomes. However, because many root-associated microbes are also sensitive to plant root traits, their responses to drought may also reflect drought-induced changes in the host phenotype. Both soil- and root-associated microbiomes under drought exhibit consistent enrichment of gram-positive bacteria and depletion of gram-negative bacteria (Acosta-Martínez *et al.* 2014; Fuchslueger *et al.* 2016; Naylor *et al.* 2017). Within those categories, however, some bacterial phyla respond to drought differently in soil versus roots (Naylor and Coleman-Derr 2018). For example, enrichment of Bacillota (formerly Firmicutes) and Actinomycetota (formerly Actinobacteria) during drought are less pronounced in soil than in root-associated microbiomes, suggesting that these phyla respond to drought-induced changes in root physiology (Santos-Medellín *et al.* 2017; Naylor *et al.* 2017; Fitzpatrick *et al.* 2018). Thus, drought impacts both soil- and root-associated microbiomes, but in different ways, owing to the influence of the plant phenotype.

Changes in soil- and root-associated microbiomes due to historical precipitation may affect plant fitness under drought. Drought-induced restructuring of root-associated microbiomes is hypothesized to be a conserved mechanism (Naylor *et al.* 2017; Xu and Coleman-Derr 2019) that supports survival of both the plant host and its symbionts (Xu *et al.* 2018). In one study, plant fitness peaked when the soil microbiome's historic moisture conditions matched contemporary experimental conditions (Lau and Lennon 2012). Additional research suggests that exposure to short-term drought creates a microbial legacy effect that moderates drought stress in plants (Kaisermann *et al.* 2017; De Long *et al.* 2019) and strengthens positive plant-soil feedbacks, although many such patterns were species-specific (Buchenau *et al.* 2022). Thus, how historical

precipitation patterns condition soil- and root-associated microbiomes and their relevance to plant fitness under drought stress is an open question.

Another open question is how historical sympatry between a plant species and the soil microbiome influences their interactions during drought. For example, drought-stressed *Arabidopsis thaliana* performed better in soil collected from a habitat where the plant had naturalized, compared to soils from a maize field and a forest stand of *Pinus ponderosa* (Zolla *et al.* 2013). Conversely, historical sympatry can be detrimental in agricultural systems: soil-dwelling plant pathogens tend to accumulate over time in monocultures (Sumner *et al.* 1990; Strom *et al.* 2020; Wachowska and Rychcik 2023), leading to negative plant-soil feedbacks (Cesarano *et al.* 2017; Jing *et al.* 2022) that drive lower plant performance in sympatric soils. Agricultural practices such as tillage and irrigation, however, may obscure some of these patterns as has been observed previously (Raaijmakers *et al.* 2009; Putten *et al.* 2016; Delavaux *et al.* 2021). Thus, we designed an experiment to assess plant fitness under a contemporary drought when grown in sympatric and non-sympatric conditioned soils from different land use types and historic precipitation regimes.

Our experiment tested how soil microbiomes with different precipitation and land use legacies impacted *Zea mays* L. (maize) under drought stress. We collected four native prairie soils across an east-west precipitation gradient in Kansas (Figure 1). For two of these sites, we also collected soil from adjacent agricultural grain fields; these paired samples represented two land use regimes with differing degrees of sympatry with maize. We inoculated maize seedlings with these soil communities and measured plant growth during our experimental drought. Specifically, we: **1**) characterized plant phenotype and microbiome responses to drought, **2**) tested how soil microbiome histories (precipitation and land use type) affected maize growth, and **3**) identified

microbial taxa that were associated with plant growth. Our results suggest that both historical and experimental drought shape soil microbiomes' interactions with maize.

Material and Methods

Soil inoculum sources and preparation

Soil samples were collected in May 2019 from 4 prairie sites and 2 agricultural sites across a steep precipitation gradient in Kansas, USA (Figure 1). Western prairie sites (SVR and HAY) are predominantly short- to mixed-grass prairies (e.g., *Bouteloua* spp.), while eastern sites (TLI and KNZ) are dominated by tallgrass prairie species (e.g., *Andropogon gerardi*, *Schizachyrium scoparium*, *Panicum virgatum*, etc.). Agricultural fields were irrigated according to a conventional grain cultivation management regime (maize and soybean rotation), whereas prairie soils were never tilled or irrigated. From each field site, soil was collected from each corner and the center (five sub-samples per site), sampling to an approximate depth of 60 cm. Soil sub-samples were homogenized and sieved to remove rocks and plant material and then stored in plastic bags at 4ºC until use, approximately four months after collection.

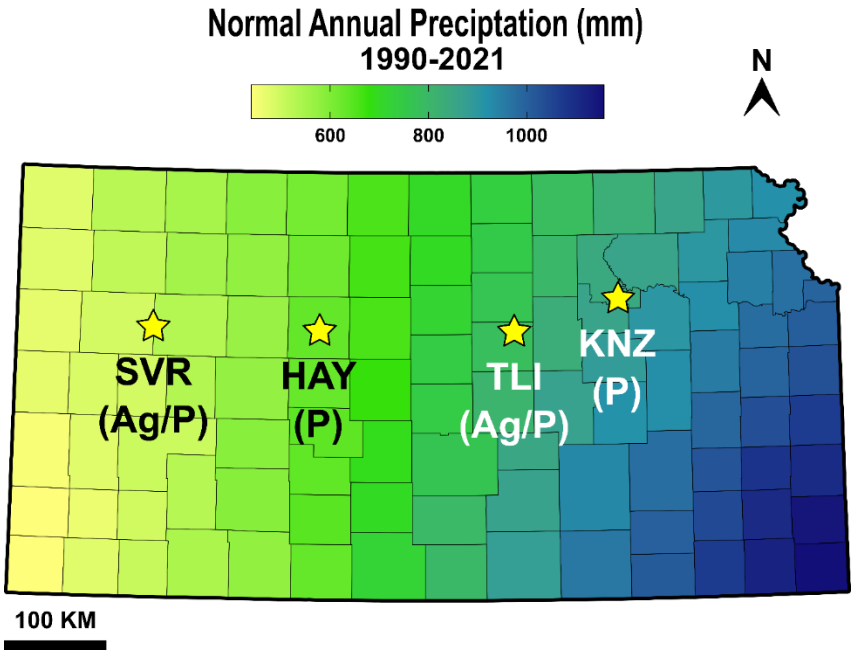

Figure 1. Kansas precipitation gradient. Soil samples were collected from either agricultural grain fields (Ag) or native prairies (P) (land use types) at four locations in Kansas along an increasing precipitation gradient (Smoky Valley Ranch [SVR] prairie [latitude 38.8665, longitude -100.9951], SVR grain field [38.8791, -100.9828], Hayes [HAY] prairie [38.8355, -99.3033], The Land Institute [TLI] grain field [38.6943, -97.5912], TLI prairie [38.9698, -97.4690], and Konza [KNZ] native prairie [39.1056, -96.6099]).

Inocula were prepared by mixing 20 g of each soil into 100 mL 1x phosphate-buffered saline (PBS) and 0.0001% Triton X-100. After settling, the soil slurries were filtered through Miracloth (22-25 µm pore size; Calbiochem, San Diego, CA, USA) and then centrifuged for 30 minutes (3000 x g). After discarding the supernatant, the microbial pellets were resuspended in 20 mL 1x PBS and kept shaking for aeration until use, later that day. Each final inoculum consisted of 10 mL of the resuspended pellet in 1 L 0.5X Murashige and Skoog basal salt mixture (MS; Sigma-Aldrich, Darmstadt, Germany). A control treatment was made by adding 10 mL sterile 1x PBS into 1 L 0.5X MS.

Planting, inoculation, and greenhouse setup

To increase the generalizability of our results, two genotypes of *Zea mays* L. (maize) were used: B73 and Mo17 (Schultz *et al.* 2022). In a laminar flow hood, seeds were surface sterilized by submerging in 70% ethanol, then 5% NaClO, followed by three rinses with sterile water. To avoid confounding effects of soil physicochemical properties, autoclaved calcined clay ("Pro's Choice Rapid Dry"; Oil-Dri Corporation, Chicago, IL) was used as the growth medium. Seeds were planted one inch deep in 107mL "cone-tainers" (Stuewe & Sons Inc., Tangent, OR, USA) with a sterilized cotton ball pushed to the bottom to prevent clay from passing through drainage holes. Approximately 100mL of sterilized calcined clay was used per cone-tainer. The day after planting, cone-tainers were assigned randomly to treatments, inoculated with 25 mL of one of the six soil inocula (or the sterile control), and placed two inches apart in randomized complete blocks

containing the 24 treatment combinations, one of four controls, and three additional replicates (Figure S1A). Overall, each combination of treatments (drought treatment × soil microbiome × genotype) was replicated 29 to 31 times across 27 randomized blocks. Plants were grown in a temperature-controlled greenhouse (23/20 ºC day/night, respectively) at the University of Kansas (Lawrence, KS, USA) arranged under growth lights (250 W Sun Systems Compact Cool fluorescent lamps) to supplement natural light for 13 hours/day during the experiment (January-March 2020).

Monitoring and harvesting plants

All plants received 30 mL of reverse osmosis water twice weekly until emergence. After emergence, "well-watered" plants continued twice-weekly watering while "droughted" plants were watered every 8-12 days. Plant height was measured weekly to the nearest 0.25 cm on the tallest fully expanded leaf held parallel to the stem. Plants were sequentially harvested to measure biomass at one of three time points during the experiment: 100 plants on day 24 and day 39, and the remainder (n=344) on day 50 (Figure S1B). Calcined clay was removed from roots by hand. Shoot and root fractions were separated and oven-dried at 65 ºC to a constant weight. Before drying, one nodal root (from the uppermost soil-borne root whorl) per plant was collected and stored at -80 ºC until DNA extraction.

Phenotypic analysis

All statistical analysis for phenotypic and microbiome data (see below) was conducted in R v3.6 (R Core Team 2021). Differences among group means were assessed using analysis of variance (ANOVA) with Type III sums of squares in the car v3.0.13 (Fox and Weisberg 2019) or lmertest v3.1.3 packages (Kuznetsova *et al.* 2017) with post-hoc comparisons made using the emmeans package v1.7.4.1 (Lenth *et al.* 2020). Assumptions of all models were checked by

inspecting model residuals (Harrison *et al.* 2018). Dry shoot and root mass were converted to accumulation rates (g/day) to account for the variable number of growing days plants experienced post-emergence. The lme4 package v1.1.29 (Bates *et al.* 2015) was used to fit a generalized linear mixed model for emergence (binary) and linear mixed models for other growth responses (continuous). Models used the following formula (*growth response* ~ *Inoculum* × *Treatment* × *Genotype*) with all possible interactions included. Experimental block was treated as a random effect with time point included as an additional random effect in the root/shoot ratio model. Root/shoot ratio was log-transformed and both shoot and root mass rate were square-root-transformed to meet the assumptions of ANOVA.

Models were also fit using climate metrics to test for linear relationships between plant growth and climatic conditions from the soil microbiome origin sites. Monthly precipitation, evapotranspiration, Palmers Drought Severity Index (PDSI), and soil moisture values were extracted from TerraClimate database (Abatzoglou *et al.* 2018), selecting the closest 4x4 km grid cell to each site. Annual normals (30-year averages; Figure S2) were calculated for each metric, PDSI was calculated as a monthly average to reduce autocorrelation, and an aridity index was calculated by dividing normal annual precipitation by evapotranspiration.

DNA extraction and library preparation

Nodal roots were freeze-dried for 48 hours (FreeZone lyophilizer; Labconco, Kansas City, MO, USA) and ground to powder with a HT Lysing Homogenizer (OHAUS, Parsippany, NJ, USA). Each ground root sample was mixed into 800 µL lysis buffer (1M Tris pH=8.0; 0.5 mM NaCl; 10 mM EDTA) and transferred to 96-well plates containing 500 µL 1 mm garnet rocks per well (Biospec Products, Bartlesville, OK, USA), after which DNA purification proceeded via bead-beating and chemical lysis as previously described (Wagner *et al.* 2020). DNA from soil and

freshly generated inocula samples was extracted in December 2022 using the same protocol but omitting the lyophilization step and placing 250 mg soil or 800 µL inoculum directly into a garnet plate.

Amplicon sequencing libraries were prepared using established protocols and PCR conditions (Wagner *et al.* 2020). Briefly, we targeted the V4 region of the 16S SSU rRNA gene for bacteria/archaea using 515F-806R primers (Apprill *et al.* 2015; Parada *et al.* 2016) and the ITS1 region for fungi using ITS1f and ITS2 primers (White *et al.* 1990; Gardes and Bruns 1993). Both amplicons were amplified separately using an initial PCR and then barcoded via a second index PCR. Amplicons were sequenced (2x250 bp) on a NovaSeq 6000 SP flow cell (Illumina, San Diego, CA, USA). Each "batch" of 96 samples (n=6) remained together throughout DNA extraction, amplification, and sequencing.

Bioinformatic processing

Sequence processing and quality filtering was conducted using an established workflow (Wagner *et al.* 2020). Briefly, Cutadapt v2.3 (Martin 2011) was used to remove primers and demultiplex sequences into 16S and ITS sequence files. DADA2 v1.14.1 (Callahan *et al.* 2016) was used to denoise reads, merge paired-end sequences, dereplicate, and remove chimeric sequences. For 16S reads, the forward and reverse were truncated to 220 and 170bp, respectively and filtered based on the maximum number of expected errors of eight and nine bp per read, respectively. ITS reads were processed using DADA2 in an identical manner, except reads were not truncated to preserve biologically relevant length variation. Forward and reverse 16S and ITS reads were then used separately to learn the error rate prior to dereplication of reads into Amplicon Sequence Variants (ASVs) and merging of pair-end reads. Taxonomy was assigned to the resulting ASVs by a naïve Bayesian classifier (Wang *et al.* 2007) trained on the 11.5 release of the

Ribosomal Database Project (Callahan 2017) for bacteria and the 01.12.2017 release of the UNITE database (UNITE Community 2017) for fungi. Phyloseq v1.40.0 (McMurdie and Holmes 2013) was used to remove host sequences (chloroplast and mitochondria; 0.37% of 16S reads) and ASVs unassigned to a kingdom. Chao1 richness and diversity indices (Shannon and Inverse Simpson) were calculated before the removal of ASVs not observed ≥25 times in ≥5 samples and samples with <400 reads (309 bacterial and 188 fungal samples); 98.1% and 95.2% of reads remained after host filtering and thresholding (bacterial and fungal reads, respectively). Finally, ASV counts were normalized via a centered-log-ratio (CLR) transformation using the ALDEx2 package v1.28.1 (Fernandes *et al.* 2014; Gloor *et al.* 2017). Due to low replication and low sequencing depth at the earlier timepoints, we analyzed only microbiome samples from the last time point. This retained 204 bacterial (mean read depth 127,588 ± SE 14,559) and 133 fungal samples (39,334 ± 7,636).

Microbiome Analysis

To test the similarity of inocula to their soils of origin, a linear model was fit for each alpha diversity metric with collection site, substrate (soil *vs.* inoculum), and sequencing depth (Z-transformed) as main effects. Community composition was assessed by permutational multivariate analysis of variance (PERMANOVA) and constrained partial redundancy analysis (RDA). For PERMANOVA, the *adonis2()* function from the vegan package v2.6.2 (Oksanen *et al.* 2019) was used to model the matrix of between-sample Aitchison distances (Gloor *et al.* 2017) with collection site and substrate as main effects. The RDA was fit with the same model, removing variance attributed to log(Sequencing Depth), and visualized using an ordination plot.

To investigate root microbiome responses, a model was fit for each alpha diversity metric (*Metric ~ Soil Inoculum × Drought Treatment + Genotype*), with *Block* and *Batch* as random effects. Genotype was treated as a fixed effect without interactions to generalize results across

genotypes and increase power to detect other main effects. The CLR-transformed abundance of each genus was modeled to test responses to experimental factors. Across all models and where appropriate, p-values were adjusted to correct for multiple comparisons using a Benjamini-Hochberg correction (Benjamini and Hochberg 1995). To explore changes in community composition, a PERMANOVA model was fit (*Aitchison distance matrix ~ Soil Inoculum × Drought Treatment + Genotype*) with permutations constrained by *Batch.* Main effects were tested for homogeneity of dispersions using the vegan package. Pairwise dispersions among factor levels were assessed using a permutation test with 999 permutations constrained by *Batch.* Constrained partial redundancy analysis of the Aitchison distance matrix was conducted to remove variance attributed to *Batch* and *log(Sequencing Depth)* and to visualize the variance in microbial composition explained by experimental factors.

The machine-learning package caret v6.0.92 (Kuhn 2008) with ranger's v0.14.1 (Wright and Ziegler 2017) implementation of the random forest algorithm was used to assess how accurately roots could be classified as droughted or well-watered based on microbiome community data (bacterial and fungal, separately). Samples were randomly split into a training set (80%) and a test set (20%), with the test set withheld from the model, and used to determine the final model's performance. Hyperparameters were optimized using a grid search over minimum node size (1, 5, 10) and the number of features available at each node (10-100% of the ASVs). For each combination in the grid, classifier accuracy was used to assess performance on out-of-bag samples with 10-fold cross validation. Final predictions were made with the trained model on the withheld test set and visualized using confusion matrices. The contribution of each ASV to classification accuracy was assessed using permuted importance: mean decrease in accuracy (MDA) values were calculated for each ASV across the 10-fold cross validation. The benefits of this strategy are

twofold, in that we can assess if drought induced a predictable shift in the microbiome as a whole, as well as identify individual ASVs with the greatest differential abundance as a result of drought.

Connecting plant growth responses to microbial abundances

Linear models were used to test associations between taxon abundances and plant growth. To focus on the phenotypic variation that could not be explained by Genotype, Inoculum, Block and Batch effects, we extracted residuals from a model that contained these terms and used them as the response variable for a second model ($Growth\ Response_{residual} \sim Taxon\ abundance \times Drought\ Treatment$). *Taxon abundance* described the association of the taxon (CLR-transformed counts of bacterial families and fungal orders) with plant growth rate; the interaction term described whether the taxon's effect on plant growth differed under droughted vs. well-watered conditions. We choose family and order as the taxonomic level for testing bacteria and fungi, respectively as conservative measure to limit the number of tests, p-values were adjusted by term to account for multiple testing.

Results

Soil and inocula community composition differs across collection sites

We assessed the microbial community composition of soils and their derived inocula from the six collection sites (n=8 samples per site). Bacterial and fungal alpha diversity of soils differed across collection sites (Tables S1 and S2); bacterial diversity was highest in the westernmost prairie soil whereas fungal diversity was highest in the easternmost prairie soil (Figures S3 and S4). Additionally, community composition of both bacterial and fungal microbiomes differed among sites (Table S3; R^2=0.22-0.23; p-value<0.01). Relative abundances of bacterial phyla and fungal classes further showed site-specific patterns (Figures S4 and S5), however, few were correlated with longitude.

Relative to the original soils, the inocula had similar bacterial alpha diversity but lower fungal richness (Figure S4C-D; Tables S1 and S2). The composition of both bacterial and fungal communities also shifted between soils and their derived inocula (Figure S5-6; Table S3); however, both soil and inocula samples clustered in ordination space by collection site (Figure 2). Thus, the original soil microbial communities remained distinct from one another in the derived inocula.

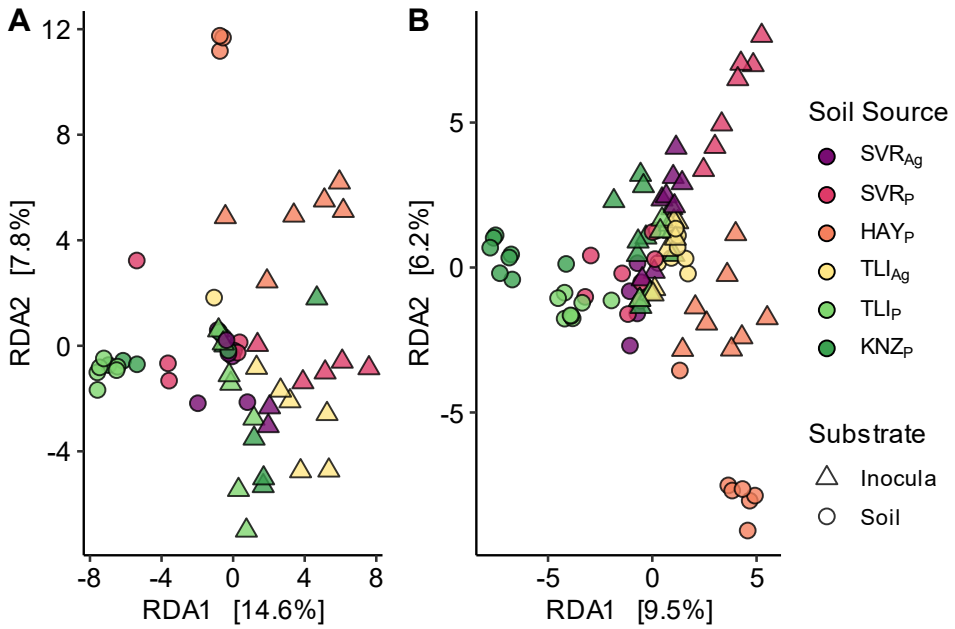

Figure 2. Soil community composition is strongly differentiated across the soil sources and substrates. Redundancy analysis for **A**) bacterial and **B**) fungal communities from soil sources used to derive soil inocula. Soil source and substrate are represented by differing colors or shapes, respectively.

Plant responses to soil microbiomes vary across genotype and drought treatment

We found no evidence that soil inocula impacted emergence rates (*p*-value = 0.37, Pearson's χ^2 test; Table S4), however, maize genotype B73 (82.5%) emerged more successfully than Mo17 (62.0%; *p*-value=0.05, Pearson's χ^2 test). Post-emergence, both drought treatment and maize genotype affected plant growth responses (Table 1). Drought decreased both shoot and root

mass accumulation rates (Figure 3A-B; *p*-value=<0.01) and increased root/shoot ratio (Figure 3C; *p*-value<0.01). These traits also differed between genotypes, with Mo17 investing more into root growth than B73 (Figure S7; *p*-value=<0.01). Shoot mass rate was the only trait that responded to soil inoculum (Table 1; *p*-value=<0.01); this effect was driven by the 'TLI$_P$' inoculum, which slowed the accumulation of root mass.

Table 1. Type three analysis of variance (ANOVA) for plant growth responses.

		sqrt(Shoot mass rate)		**sqrt(Root Mass Rate)**		**log(Root/shoot Ratio)**	
Factor	DF	*F*-value	*p*-value	*F*-value	*p*-value	*F*-value	*p*-value
Drought Treatment (DT)	1	471.39	**<0.01**	31.09	**<0.01**	216.09	**<0.01**
Genotype (G)	1	32.57	**<0.01**	30.34	**<0.01**	111.01	**<0.01**
Soil Inoculum (SI)	5	3.42	**<0.01**	0.4	0.85	2.14	0.06
DT x G	1	0.11	0.74	2.36	0.12	0.15	0.7
DT x SI	5	1.3	0.26	1.18	0.32	0.99	0.42
G x SI	5	1.95	0.09	0.64	0.67	2.65	**0.02**
DT x G x SI	5	0.77	0.57	0.22	0.95	0.12	0.99

Bold values denote significant effects, *p*-value<0.05

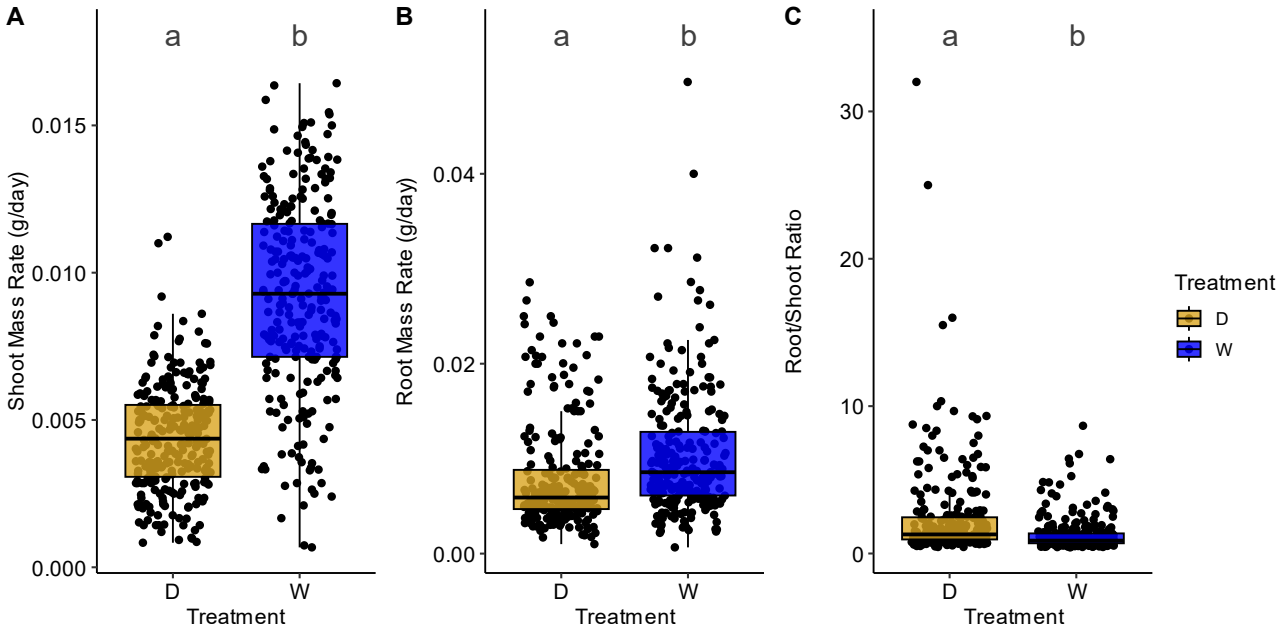

Figure 3. Shoot and root growth vary across drought treatment. The effect of drought treatment on **A)** shoot mass rate, **B)** root mass rate, and **C)** root/shoot ratio. Boxplot hinges represent the 1st and 3rd quartiles; whiskers represent 1.5 times the interquartile range; letters above

box plots denote significant differences in estimated marginal means (*p*-value=<0.01; see table 1 for full ANOVA table).

We observed no evidence of interactions between drought treatment and soil inoculum on plant growth responses. However, inoculum interacted with genotype to influence root/shoot ratio (Table 1; *p*-value=0.02). Mo17 displayed greater root/shoot ratios than B73 across all inocula, although the magnitude of this difference varied (Δ_{emmean} 0.176-0.493; *p*-value=0.02-<0.01). Land use type impacted B73 growth, as shoot mass accumulated more quickly than Mo17 when inoculated with three of the four prairie soil microbiomes ('SVR_P' *p*-value=<0.01, 'HAY_P' *p*-value=<0.01, 'TLI_P' *p*-value=0.03, 'KNZ_P' *p*-value=0.27) but not with agricultural soil microbiomes ('SVR_{Ag}' *p*-value=0.33, 'TLI_{Ag}' *p*-value=0.12). Thus, the effect of soil microbial communities on maize growth generally depended on plant genotype, but not on the drought treatment.

Root microbiomes and community responses to drought modulated by soil inoculum

Drought treatment and soil inocula collection site impacted the richness and diversity of root-associated bacterial and fungal communities (Tables S5 and S6). Drought increased Chao1 richness of bacterial communities (Tables S5 and S6; *p*-value=0.01) but affected neither Shannon nor Inverse Simpson diversity. In contrast, Shannon and Inverse Simpson fungal diversity increased under drought conditions, particularly for plants that received the 'TLI_P' inoculum (Figure 1; Table S6; *p*-value=0.01–0.02).

Bacterial community composition depended on the soil inoculum (Table 2; R^2=0.05, *p*-value=<0.01, PERMANOVA) and drought treatment (Figure 4A; R^2=0.01, *p*-value=<0.01, PERMANOVA). We found no evidence that bacterial community dispersion differed among treatments, genotypes, or inocula (*p*-value=>0.05, Multivariate Levene's test). Redundancy analysis aligned with PERMANOVA results: soil inoculum and drought treatment explained the

largest proportions of variance (6.09% and 1.57%; Figure S8 and 4B, respectively), while genotype explained <1% of variance (Figure S9). Several genera were responsive to the drought treatment, *Arthobacter*, *Cupriavidus*, *Nitrospirillum*, *Sphingomonas*, and *Xanthobacter* (q=1.3e^{-3} - 1.7e^{-5}). *Arthobacter* and *Nitrospirillum* were enriched under drought conditions (65.3% and 71.0% increase in relative abundance, respectively) whereas *Cupriavidus*, *Sphingomonas*, and *Xanthobacter* were enriched under well-watered conditions (73.3%, 62.4%, and 90.2%, respectively).

Table 2. Permutational Multivariate ANOVA (PERMANOVA) table bacterial community composition of maize nodal roots.

Factor	DF	SS	R^2	*F*-value	*p*-value
Genotype (G)	1	4109	0.01	1.23	0.21
Soil Inoculum (SI)	5	34055	0.05	2.04	**<0.01**
Drought Treatment (DT)	1	7483	0.01	2.24	**<0.01**
SI x DT	5	16011	0.02	0.96	0.52
Residual	185	617812	0.91		

Bold values denote significant effects, *p*-value<0.05

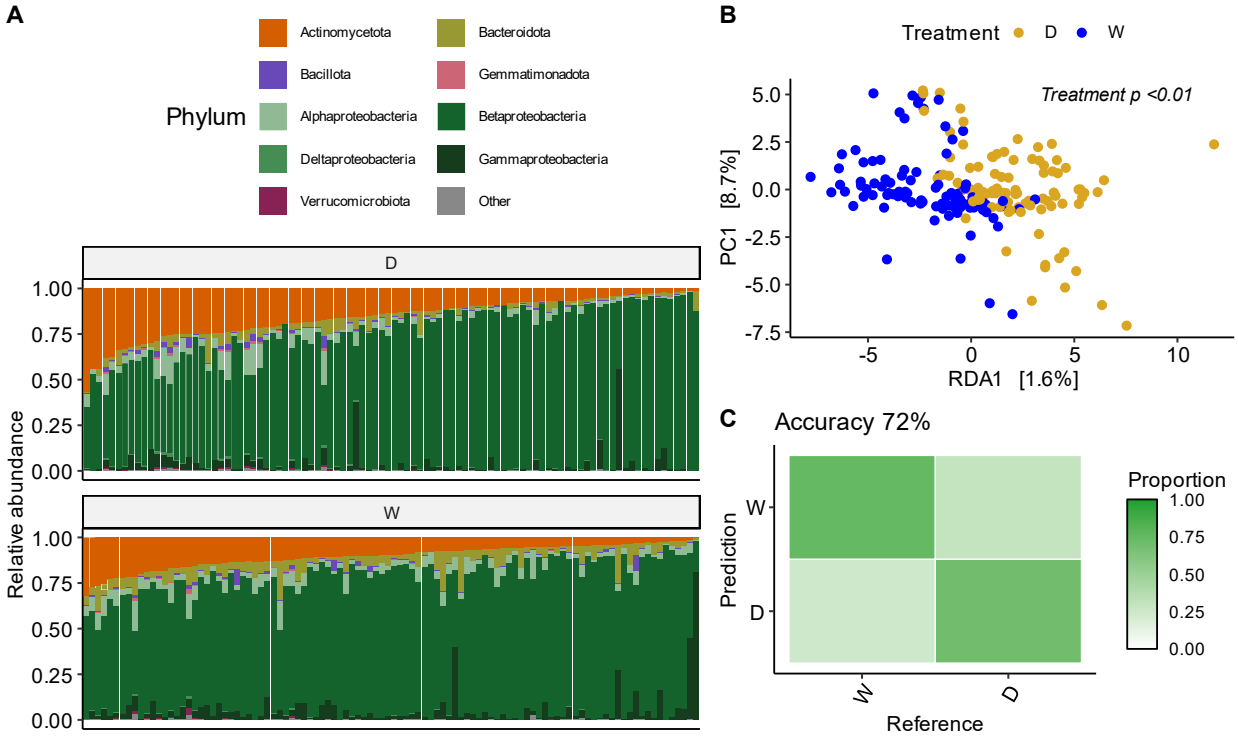

Figure 4. Bacterial community composition across drought treatment. A) Bacterial and taxonomic barplots for drought (D) and well-watered (W) plants. Each sample is represented by a single line with the relative abundance (non CLR transformed data) of each phylum displayed by color. **B)** Redundancy analysis on bacterial communities fit by drought treatment. Redundancy analysis was conditioning for sequencing batch and log transformed usable reads per sample. **C)** Confusion matrix depicting the classification accuracy of a random forest classifier predicting drought treatment trained on bacterial communities. Above the confusion matrix balanced accuracy is shown, for additional classifier statistics see Table S8

In contrast, drought treatment did not alter relative abundances of any fungal genera, nor overall root fungal community profiles (Figure 5A). Variance in fungal community composition was mostly due to initial soil inoculum source (Figure S10; Table 3; R^2=0.09, *p*-value=<0.01). As observed for bacterial communities, neither drought treatment, maize genotype, nor soil inoculum source affected fungal community dispersion (*p*-value=>0.05, Multivariate Levene's test). Drought and maize genotype each explained <1% of the variance in fungal community composition (Figure 5B and S11, respectively). Thus, while root-associated bacterial community composition responded to drought treatment, we observed no trend for fungal community composition.

Table 3. PERMANOVA table for fungal community composition of maize nodal roots.

Factor	DF	SS	R^2	*F*-value	*p*-value
Genotype (G)	1	774	0.01	1.01	0.28
Soil Inoculum (SI)	5	9152	0.09	2.40	**<0.01**
Drought Treatment (DT)	1	693	0.01	0.91	0.42
SI x DT	5	4198	0.04	1.10	0.22
Residual	116	88478	0.86		

Bold values denote significant effects, *p*-value<0.05

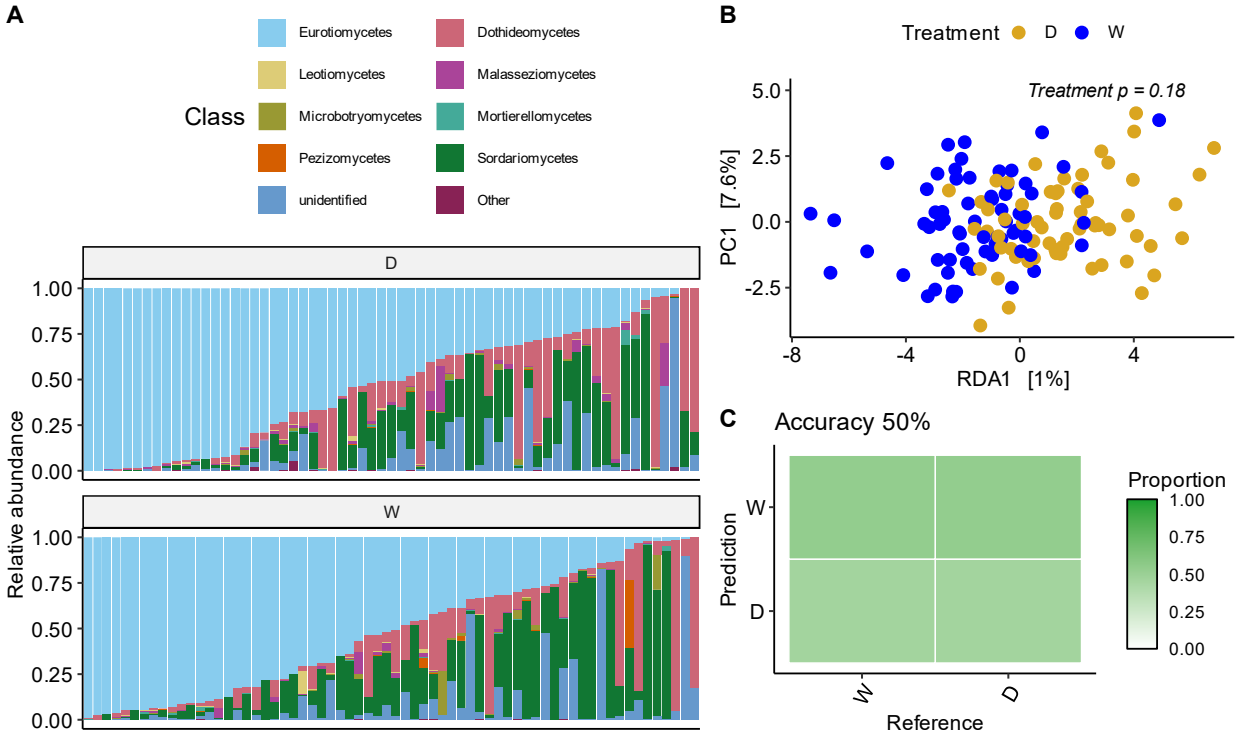

Figure 5. Fungal community composition across drought treatment. A) Fungal taxonomic barplots for drought (D) and well-watered (W) plants. Each sample is represented by a single line with the relative abundance (non CLR transformed data) of each class displayed by color. **B)** Redundancy analysis on fungal communities fit by drought treatment. Redundancy analysis was conditioning for sequencing batch and log transformed usable reads per sample. **C)** Confusion matrix depicting the classification accuracy of random forest a classifier predicting drought treatment trained on fungal communities. Above the confusion matrix balanced accuracy is shown, for additional classifier statistics see Table S9.

Identification of bacterial and fungal ASVs responding to drought

Our random forest models showed greater accuracy in predicting the drought treatment of a given sample when trained on bacterial vs fungal communities (Figures 4C&5C). Two bacterial ASVs from the genus *Sphingomonas* (Pseudomonadota) were the top two features contributing to prediction accuracy of the random forest classifier when attempting to predict drought treatment, with a mean decrease in accuracy (MDA) of 2.88% and 0.59% when withheld from the model (Figure 4C and S12-13). In other words, these two bacterial ASVs contributed to ~3.5% increase of model accuracy in predicting drought and were positively correlated with one another (*p*-

value=<0.01; r=0.521 Pearson test). These *Sphingomonas* ASVs were depleted in droughted plants relative to well-watered plants (10.8% decrease in relative abundance). In contrast, we did not detect any fungal ASVs that were differentially abundant in response to drought treatment, nor any that contributed to random forest classifier accuracy with MDA value >0.5% (Figure 5C and S14-15).

Connecting plant growth responses to bacterial and fungal communities

Soil inocula derived from collection sites across Kansas had only a small impact on plant growth responses (Table 1; Figure 6A and S15), with no single site showing significantly improved growth over other sites or the control. Examining the prairie sites spanning the east-west precipitation gradient, we detected an interaction between mean annual precipitation and drought treatment (Figure 6B; *p*-value=0.04). The shoot mass accumulation rate of well-watered plants was negatively associated with mean annual precipitation of the soil microbiome collection site (slope = $-2.88e^{-6}$ g/day/mm precipitation) whereas droughted plants displayed a weak positive association (slope = $4.53e^{-7}$ g/day/mm precipitation). Put another way, counterintuitive to expectations, plants that experienced drought benefited from microbiomes from historically wetter soils, while the opposite was true for well-watered plants in the experiment (we discuss this striking pattern below). This pattern was consistent when substituting longitude and other climatic metrics (PDSI, aridity index, and soil moisture) for mean annual precipitation (Figure S17; *p*-values = 0.03, 0.03, 0.06, and 0.18, respectively). Notably, B73 and Mo17 exhibited contrasting associations with mean annual precipitation across the Kansas precipitation gradient (Figure 6C; *p*-value=0.02; Slope=$-2.94e^{-6}$ and $5.10e^{-7}$, respectively).

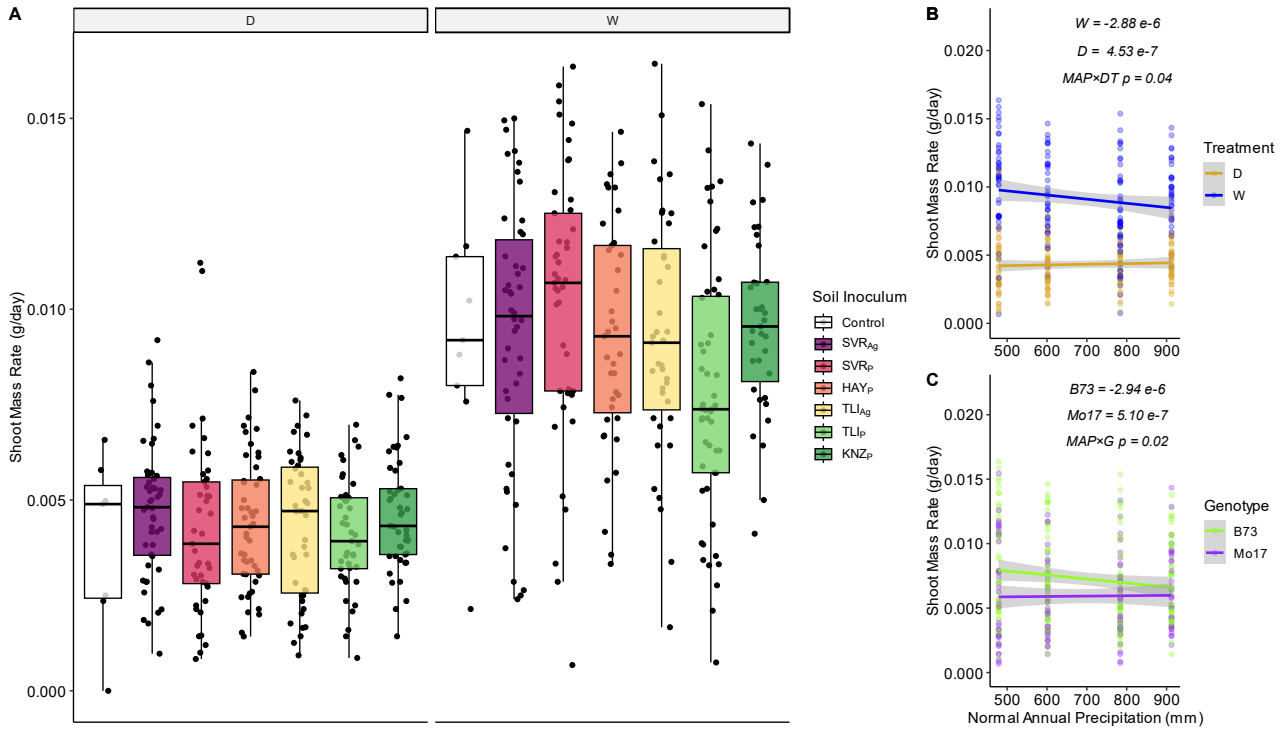

Figure 6. Shoot and root growth responses by soil inoculum. Boxplots are colored by soil inoculum for **A)** shoot mass rate, **B)** root mass rate, and **C)** root/shoot ratio (four R/S data points were removed to reduce the y axis range and aid in visualization). Separate facets represent drought (D) and well-watered plants (W). Boxplot hinges represent the 1st and 3rd quartiles; whiskers represent 1.5 times the interquartile range. **D-E)** trend lines for shoot mass rate of significant interactions of mean annual precipitation (last climate normal 1991-2020) with drought treatment and genotype, respectively, for plants inoculated with prairie soils. For each regression line, grey shading represents the 95% confidence interval.

We identified bacterial and fungal taxa correlated with promotion or suppression of plant growth. Overall, 13 bacterial families showed a significant positive (6/13) or negative (7/13) effect on shoot mass accumulation rate (Table 4). These represented only a few phyla (6 Actinomycetota, 5 Pseudomonadota, and 2 Bacillota) and were predominantly gram positive (8/13). Two of the identified families (Corynebacteriaceae and Streptococcaceae) interacted with drought treatment, indicating that their effect on shoot mass rate was modulated by the amount of water the plant received. The abundances of Corynebacteriaceae and Streptococcaceae were negatively correlated with shoot mass rate in well-watered plants but not in droughted plants (Figure S18). Using the

same analysis framework, root mass rate was not associated with any bacterial families, possibly because its variance decreased over time as roots expanded to fill the entire container regardless of treatment or inoculum (Figure S19). In addition, bacterial families that correlated with root/shoot ratio were simply a subset of the bacterial families identified for shoot mass accumulation rate. For fungi, only shoot mass rate showed significant correlations with the abundance of fungal orders (Table 5). All three significant fungal orders (Hypocreales, Malasseziales, and Sporidiobolales) were positively correlated with shoot growth regardless of the water regime applied. Similar results were found at lower taxonomic levels as well for bacteria and fungi (Table S10-11).

Table 4. Bacterial families associated with square root transformed shoot mass rate.

Taxon	Model Term	R	X	PVE_{Res}	Rel. Abund.	*q*
Lactobacillaceae	Abundance	3.92E-04	-1.52E-02	3.6	0.14	3.74E-02
Nocardiaceae	Abundance	2.84E-04	-1.43E-02	3.63	0.02	1.30E-02
Microbacteriaceae	Abundance	1.11E-04	-1.51E-02	5.14	1.17	1.69E-02
Sinobacteraceae	Abundance	1.03E-04	-1.46E-02	2.31	0.05	6.45E-05
Micrococcaceae	Abundance	2.58E-05	-1.48E-02	2.77	8.06	4.08E-04
Alcaligenaceae	Abundance	1.58E-06	-1.42E-02	3.04	0.05	4.54E-03
Corynebacteriaceae*	Abundance	-1.19E-04	-1.40E-02	6.38	0.01	4.26E-04
Sphingomonadaceae	Abundance	-1.21E-04	-1.25E-02	5.49	1.18	1.69E-02
Streptococcaceae*	Abundance	-1.61E-04	-1.39E-02	5.52	0.02	5.02E-03
Rhodospirillaceae	Abundance	-4.46E-04	-1.19E-02	5.54	0.08	4.08E-04
Dietziaceae	Abundance	-6.54E-04	-1.38E-02	4.97	<0.01	3.37E-02
Beijerinckiaceae	Abundance	-8.49E-04	-1.46E-02	2.76	<0.01	4.08E-04
Actinomycetaceae	Abundance	-1.85E-03	-1.47E-02	2.18	<0.01	3.19E-04

*Corynebacteriaceae and Streptococcaceae both show significant interactions between the family abundance and drought treatment, these are presented in Figure S11.

Table 5. Fungal orders associated with square root transformed shoot mass rate.

Taxon	Trait	Model Term	R	X	PVE_{Res}	Relative Abundance	*q*
Hypocreales	SMR	Abundance	4.75E-05	-1.42E-02	3.28	19.23	4.68E-02
Malasseziales	SMR	Abundance	9.97E-05	-1.42E-02	2.92	1.22	4.86E-02
Sporidiobolales	SMR	Abundance	6.36E-04	-1.34E-02	4.87	0.66	1.47E-02

Discussion

Understanding plant-microbiome interactions under drought stress is critical to safeguard agricultural systems in the face of global climate change. In this study, we measured the growth of maize seedlings under experimental drought after inoculation with soil microbiomes from across a natural precipitation gradient in Kansas. Under drought stress, we observed phenotypic differences in maize resource allocation and the restructuring of bacterial, but not fungal, root microbiome communities. Following the stress gradient hypothesis (Bertness and Callaway 1994) we expected drought-stressed maize seedlings to perform better in the presence of microorganisms from historically dry soils, where chronic drought stress would have fostered positive interactions with neighboring plants. We detected an effect of historical precipitation exposure on prairie soil microbiomes' interactions with plant hosts during drought treatment. Notably, opposite of that predicted by the stress gradient hypothesis: prairie soils from historically wetter locations increased maize biomass under experimental drought more than soils from historically dry locations. Historical land use at the soil microbiome collection site also impacted growth of B73, which accumulated shoot mass more rapidly when grown with prairie soil inocula than agricultural soil inocula. Deeper analysis revealed several bacterial and fungal taxa that were associated with plant growth promotion or suppression and that were modulated by the experimental drought.

Plant and microbiome responses to drought

In our experiment, maize displayed phenotypic tradeoffs in response to drought. Drought-treated plants increased root growth relative to shoot growth, resulting in shorter plants over the course of the experiment. This supports our understanding of plant responses to drought, as plants prioritize root over shoot growth (Sharp and Davies 1979; Lynch *et al.* 2014), favoring deeper and often denser root systems in order to obtain sufficient water (Zhan *et al.* 2015; Gao and Lynch

2016; Sebastian *et al.* 2016). These phenotypic changes in root growth, along with direct effects of water limitation in the soil, contributed to the responses of the root microbiomes in our study.

Drought altered the bacterial communities of maize roots, although the magnitude of compositional change within our study was small (R^2=0.01) relative to other studies (R^2=0.04-0.10) (Santos-Medellín *et al.* 2017; Naylor *et al.* 2017; Fitzpatrick *et al.* 2018; Xu *et al.* 2018). Similar to previous studies (Xu and Coleman-Derr 2019), we observed a depletion of gram-negative and an enrichment of gram-positive bacteria in response to drought, likely relating to the desiccation resistance provided by the single thick peptidoglycan cell wall of gram-positive bacteria (Manzoni *et al.* 2012). Enrichment of Actinomycetota during drought tends to be more pronounced in root-associated microbiomes than in soil, suggesting that shifts in plant root physiology also play a role (Naylor and Coleman-Derr 2018; Xu and Coleman-Derr 2019); however, the specific root traits driving this effect are unknown. During drought, root exudate quantity is generally maintained or increased (Henry *et al.* 2007; Preece and Peñuelas 2016; Karlowsky *et al.* 2018), but the stronger changes in exudate composition (Svenningsson *et al.* 1990; Canarini *et al.* 2016; Calvo *et al.* 2017) may contribute to the root microbiome drought response (Zhalnina *et al.* 2018). In *Sorghum*, for instance, drought-induced changes in root exudate composition and iron homeostasis contribute to Actinomycetota enrichment in the rhizosphere (Xu *et al.* 2018, 2021).

Fungal communities of maize roots were less sensitive to drought relative to their bacterial neighbors. While drought increased root fungal diversity in the plants inoculated with the TLI prairie soil inoculum, it did not significantly affect overall fungal community composition. Machine learning classification by drought treatment further illustrated this difference: when trained on bacteria, we achieved 72.5% balanced accuracy, while for fungi, we achieved only 50%.

Indicating bacterial communities responded in a predictable manner to drought, whereas fungal communities were similar between well-watered and drought plants. This cross-kingdom difference agrees with previous reports, as both free living and root-associated fungal communities tend to tolerate desiccation (de Vries *et al.* 2012; Furze *et al.* 2017). The observed difference in survival between bacteria and fungi under drought may relate to both the vegetative and dormant growth forms of fungi: compared to bacterial cells, fungal hyphae comprise most vegetative growth and can cross air-gaps within dry soil in search of resources (Griffin 1985; Manzoni *et al.* 2012), and dormant spores are generally desiccation-resistant (Wyatt *et al.* 2013).

Historical precipitation, soil community legacies, and their impact on plant drought tolerance

Our hypothesis that historical precipitation patterns would impart legacy effects on soil microbiomes that influence plant growth under drought stress was supported. Bacterial and fungal compositional differences were apparent among the soils and inocula from sites across a steep precipitation gradient in Kansas (Figures 1&2). In the four soils from prairie sites, we found a significant interaction for shoot mass rate between mean annual precipitation of soil inoculum source and drought treatment. This pattern was further supported when examining alternative climate metrics (PDSI, aridity index, and soil moisture).

Interestingly, we found that plants performed better when the historic conditions of inocula were opposite from the contemporary conditions. The reason for this surprising result is not immediately clear, but there are several possible explanations. Contemporary well-watered conditions may have relaxed the fitness consequences of expression of microbial traits that are critical under drier environments. For instance, microorganisms counteract the physiologic stress of drought by accumulating solutes, which reduces their internal water potential as a mechanism to avoid desiccation (Harris 1981). The accumulation of solutes requires considerable energy

expenditure and constitutes a large sink of C and N resources (Killham and Firestone 1984; Schimel *et al.* 1989, 2007). The contemporary well-watered conditions relax these costly solute needs, perhaps allowing resources to be reallocated to functions that are beneficial to plants. Another possibility is that soils from historically wetter sites generally possess greater microbial biomass and diversity (Neilson *et al.* 2017; Araya *et al.* 2020; Wan *et al.* 2021), which is predicted to promote positive interactions and improved community function (Hooper *et al.* 2005). We found this to be the case for fungi, where our wettest prairie site showed the highest diversity, but this was less consistent for bacterial communities (Figure S3-4). A third potential explanation involves the balance of beneficial and pathogenic microbes in the soil community. Pathogen richness in soil, root, and shoot microbiomes is often positively associated with mean annual temperature and precipitation (Větrovský *et al.* 2019; Delgado-Baquerizo *et al.* 2020; Chen *et al.* 2021). Thus, soil communities from historically dry sites may have relatively fewer plant pathogens, resulting in greater plant performance under contemporary well-watered conditions. We cannot distinguish between these possible explanations using the data in hand; however, a future experiment that leverages rain exclusion structures to manipulate precipitation for a given site could effectively explore changes in diversity and the balance of beneficial, neutral, and pathogenic microbes.

Historical sympatry between a plant species and the soil microbiome may affect performance under drought conditions for the host plant (Zolla *et al.* 2013; Kaisermann *et al.* 2017). Positive plant-soil feedbacks are generally expected to strengthen under drought conditions (Beals *et al.* 2020; Veresoglou *et al.* 2022), but this effect can vary strongly by plant species and functional group (Hassan *et al.* 2021; Lozano *et al.* 2022). However, agricultural practices (e.g., irrigation and tillage) might weaken historical drought legacies, and in turn reduce positive interactions (Bertness and Callaway 1994). Furthermore, repeated growth of a crops in

monoculture in one location, even in rotation with another species, frequently results in negative feedbacks driven by soil microbial communities (Bennett *et al.* 2012; Peralta *et al.* 2018; G Wang *et al.* 2021). Therefore, we expected that maize inoculated with agricultural soil microbiomes (*i.e.*, from grain fields where maize has long been a dominant plant species) would perform worse under drought than plants inoculated with prairie soils that were naïve to maize. Consistent with our expectation, inoculation with prairie-derived communities increased shoot mass accumulation rate and root/shoot ratio in the maize genotype B73, relative to farm-derived communities. This finding agrees with past work showing that frequent cultivation of maize in monoculture can lead to a buildup of pathogenic microbes in the soil and stronger negative plant-soil feedbacks (Sumner *et al.* 1990; Zhang *et al.* 1998; Strom *et al.* 2020; Wachowska and Rychcik 2023). The prairie soils, naïve to maize, would have had no such buildup. This explanation is consistent with our observation that the prairie inocula improved growth only in B73, which is generally more disease-susceptible than Mo17 (Carson *et al.* 2005; Balint-Kurti *et al.* 2010; Cooper *et al.* 2018). Our results support the need for additional research to tease apart the ability of dominant plant species to condition soil microbiomes in either a beneficial or detrimental manner, and to characterize the environmental dependency of such conditioning.

Microbial taxa associated with plant growth

Multiple bacteria and fungi had abundances correlated with plant growth responses to drought, even if their impact on plant growth was small. Two bacterial families, Corynebacteriaceae and Streptococcaceae, were consistently associated with suppressed growth of well-watered but not droughted plants. Corynebacteriaceae are root endophytes of multiple plant species (Stafford *et al.* 2005; Vik *et al.* 2013) including two Antarctic endemic plants (Zhang *et al.* 2020). This family contains multiple phytopathogenic species (Dye and Kemp 1977) with some

strains specific to maize (Vidaver and Mandel 1974). Additionally, during a multi-generation experimental evolution study, Corynebacteriaceae (among other bacterial families) was consistently associated with delayed flowering in multiple plant species (Panke-Buisse *et al.* 2015). Less is known about the relevance of Streptococcaceae to plant growth. In *Zingiber officinale*, this family was significantly enriched in rhizomes with advanced stages of soft rot (Huang *et al.* 2022). However, Streptococcaceae is prevalent in soil and plants (Chuah *et al.* 2016; X Wang *et al.* 2021), typically at higher abundance in aerial plant compartments than in the rhizosphere (Minervini *et al.* 2015; Yu *et al.* 2020). Both of these families represent targets for direct manipulation and *in-planta* testing to better understand the mechanism responsible for the growth suppression we observed under well-watered conditions.

Conclusions

Water is a critical and limiting resource for plant growth as well as a functional microbiome. As maize is cultivated widely across the United States, production will have to contend with more frequent episodes of drought as the global climate warms. Engineering plant microbiomes to assist in plant resilience under drought remains an ambitious, but worthwhile goal. Our work illustrates the differential responses of root and shoot growth allocation to drought in two well-studied maize genotypes and shows that bacterial, but not fungal, microbiota undergo restructuring with drought, with decreases in the relative abundance of drought-intolerant taxa. In contrast to the stress gradient hypothesis, soil microbiomes from perennially dry environments along a natural precipitation gradient did not enhance plant growth responses under drought. Instead, plants under drought tended to produce more aboveground biomass with soil microbiomes from historically wetter sites. The bacterial and fungal groups associated with biomass can serve to direct future cultivation and *in-planta* testing on maize growth.

Acknowledgements

We thank members of the Wagner lab for helpful comments in preparing this article. In addition, we thank Zachary Harris and Nichole Ginnan for helpful discussions. This work was funded by the United States Department of Agriculture National Institute of Food and Agriculture (USDA-NIFA) grant #2022-67013-36672 to MK and MRW, National Science Foundation grant #IOS-2016351 to MRW, Novo Nordisk Foundation INTERACT project under award number NNF19SA0059360 to MK, and seed funding from the NSF under award No. OIA-1656006 to Dr. Kristin Bowman-James and matching support from the State of Kansas through the Kansas Board of Regents. We thank the University of Kansas Medical Center – Genomics Core for generating the sequence data sets. The Genomics Core is supported by the Kansas Intellectual and Developmental Disabilities Research Center (NIH U54 HD 090216), the Molecular Regulation of Cell Development and Differentiation – COBRE (P30 GM122731), The NIH S10 High End Instrumentation Grant (NIH S10OD021743) and the Frontiers CTSA Grant (UL1TR002366).

Competing Interests

The authors declare that the research was conducted in the absence of any commercial or financial relationships that could be construed as a potential conflict of interest. Any opinion, findings, and conclusions or recommendations expressed in this material are those of the authors and do not necessarily reflect the views of the United States Department of Agriculture or the National Science Foundation.

Data Availability Statement

Raw sequencing data is available on NCBI SRA under BioProject ID PRJNA913622 and SRA accessions SAMN32302538-SAMN32303072 for root-associated samples and SAMN33863891-

SAMN33864082 for soil and inoculum samples. Code to reproduce the analysis and figures are available on GitHub at https://github.com/Kenizzer/Maize_Drought_Microbiome.

Author Contributions

BAS and PMH collected soil samples across Kansas. MRK, MK, and MRW designed the experiment and collection methods. MRK performed sample collection and processing. AC and NEF performed DNA extractions and library preparations. NEF and JFS performed the data analysis. JFS wrote the first draft of the manuscript. All authors contributed to data interpretation, the writing and reviewing of the manuscript, and approved the final draft.

References

Abatzoglou J.T., Dobrowski S.Z., Parks S.A., and Hegewisch K.C. 2018. TerraClimate, a high-resolution global dataset of monthly climate and climatic water balance from 1958–2015. Sci. Data 5: 170191.

Acosta-Martínez V., Cotton J., Gardner T., Moore-Kucera J., Zak J., Wester D., and Cox S. 2014. Predominant bacterial and fungal assemblages in agricultural soils during a record drought/heat wave and linkages to enzyme activities of biogeochemical cycling. Appl. Soil Ecol. 84: 69–82.

Apprill A., McNally S., Parsons R., and Weber L. 2015. Minor revision to V4 region SSU rRNA 806R gene primer greatly increases detection of SAR11 bacterioplankton. Aquat. Microb. Ecol. 75: 129–137.

Araya J.P., González M., Cardinale M., Schnell S., and Stoll A. 2020. Microbiome Dynamics Associated With the Atacama Flowering Desert. Front. Microbiol. 10: 1–13.

Averill C., Waring B.G., and Hawkes C. V. 2016. Historical precipitation predictably alters the shape and magnitude of microbial functional response to soil moisture. Glob. Chang. Biol. 22: 1957–1964.

Bachar A., Al-Ashhab A., Soares M.I.M., Sklarz M.Y., Angel R., Ungar E.D., and Gillor O. 2010. Soil Microbial Abundance and Diversity Along a Low Precipitation Gradient. Microb. Ecol. 60: 453–461.

Balint-Kurti P.J., Yang J., Van Esbroeck G., Jung J., and Smith M.E. 2010. Use of a Maize Advanced Intercross Line for Mapping of QTL for Northern Leaf Blight Resistance and Multiple Disease Resistance. Crop Sci. 50: 458–466.

Balting D.F., AghaKouchak A., Lohmann G., and Ionita M. 2021. Northern Hemisphere drought risk in a warming climate. npj Clim. Atmos. Sci. 4: 61.

Bates D., Mächler M., Bolker B., and Walker S. 2015. Fitting Linear Mixed-Effects Models Using lme4. J. Stat. Softw. 67.

Beals K.K., Moore J.A.M., Kivlin S.N., Bayliss S.L.J., Lumibao C.Y., Moorhead L.C., Patel M., Summers J.L., Ware I.M., Bailey J.K., and Schweitzer J.A. 2020. Predicting plant-soil feedback in the field: Meta-analysis reveals that competition and environmental stress differentially influence psf. Front. Ecol. Evol. 8.

Benjamini Y., and Hochberg Y. 1995. Controlling the False Discovery Rate : A Practical and Powerful Approach to Multiple Testing. J. R. Stat. Soc. 57: 289–300.

Bennett A.J., Bending G.D., Chandler D., Hilton S., and Mills P. 2012. Meeting the demand for crop production: the challenge of yield decline in crops grown in short rotations. Biol. Rev. 87: 52–71.

Bertness M.D., and Callaway R. 1994. Positive interactions in communities. Trends Ecol. Evol. 9: 191–193.

Buchenau N., van Kleunen M., and Wilschut R.A. 2022. Direct and legacy-mediated drought effects on plant performance are species-specific and depend on soil community composition. Oikos 2022: 1–14.

Callahan B.J. 2017. RDP taxonomic training data formatted for DADA2 (RDP trainset 16/release 11.5).

Callahan B.J., McMurdie P.J., Rosen M.J., Han A.W., Johnson A.J.A., and Holmes S.P. 2016. DADA2: High-resolution sample inference from Illumina amplicon data. Nat. Methods 13: 581–583.

Calvo O.C., Franzaring J., Schmid I., Müller M., Brohon N., and Fangmeier A. 2017. Atmospheric CO 2 enrichment and drought stress modify root exudation of barley. Glob. Chang. Biol. 23: 1292–1304.

Canarini A., Merchant A., and Dijkstra F.A. 2016. Drought effects on Helianthus annuus and Glycine max metabolites: from phloem to root exudates. Rhizosphere 2: 85–97.

Canarini A., Schmidt H., Fuchslueger L., Martin V., Herbold C.W., Zezula D., Gündler P., Hasibeder R., Jecmenica M., Bahn M., and Richter A. 2021. Ecological memory of recurrent drought modifies soil processes via changes in soil microbial community. Nat. Commun. 12: 5308.

Carson M.L., Stuber C.W., and Senior M.L. 2005. Quantitative Trait Loci Conditioning Resistance to Phaeosphaeria Leaf Spot of Maize Caused by Phaeosphaeria maydis. Plant Dis. 89: 571–574.

Cesarano G., Zotti M., Antignani V., Marra R., Scala F., and Bonanomi G. 2017. Soil sickness and negative plant-soil feedback: A reappraisal of hypotheses. J. Plant Pathol. 99: 545–570.

Chen Q.L., Hu H.W., Yan Z.Z., Li C.Y., Nguyen B.A.T., Zhu Y.G., and He J.Z. 2021. Precipitation increases the abundance of fungal plant pathogens in Eucalyptus phyllosphere. Environ. Microbiol. 23: 7688–7700.

Chiang F., Mazdiyasni O., and AghaKouchak A. 2021. Evidence of anthropogenic impacts on global drought frequency, duration, and intensity. Nat. Commun. 12: 2754.

Chuah L.-O., Yap K.-P., Thong K.L., Liong M.T., Ahmad R., Shamila-Syuhada A.K., and Rusul G. 2016. Genome Sequence of “Anthococcus,” a Novel Genus of the Family Streptococcaceae Isolated from Flowers. Genome Announc. 4.

Cooper J.S., Balint-Kurti P.J., and Jamann T.M. 2018. Identification of Quantitative Trait Loci for Goss’s Wilt of Maize. Crop Sci. 58: 1192–1200.

Delavaux C.S., Schemanski J.L., House G.L., Tipton A.G., Sikes B., and Bever J.D. 2021. Root

pathogen diversity and composition varies with climate in undisturbed grasslands, but less so in anthropogenically disturbed grasslands. ISME J. 15: 304–317.

Delgado-Baquerizo M., Guerra C.A., Cano-Díaz C., Egidi E., Wang J.T., Eisenhauer N., Singh B.K., and Maestre F.T. 2020. The proportion of soil-borne pathogens increases with warming at the global scale. Nat. Clim. Chang. 10: 550–554.

Dye D.W., and Kemp W.J. 1977. A taxonomic study of plant pathogenic Corynebacterium species. New Zeal. J. Agric. Res. 20: 563–582.

Fernandes A.D., Reid J.N.S., Macklaim J.M., McMurrough T.A., Edgell D.R., and Gloor G.B. 2014. Unifying the analysis of high-throughput sequencing datasets: characterizing RNA-seq, 16S rRNA gene sequencing and selective growth experiments by compositional data analysis. Microbiome 2: 15.

Field R., Hawkins B.A., Cornell H. V., Currie D.J., Diniz-Filho J.A.F., Guégan J.-F., Kaufman D.M., Kerr J.T., Mittelbach G.G., Oberdorff T., O'Brien E.M., and Turner J.R.G. 2009. Spatial species-richness gradients across scales: a meta-analysis. J. Biogeogr. 36: 132–147.

Fitzpatrick C.R., Copeland J., Wang P.W., Guttman D.S., Kotanen P.M., and Johnson M.T.J. 2018. Assembly and ecological function of the root microbiome across angiosperm plant species. Proc. Natl. Acad. Sci. 115: E1157–E1165.

Fox J., and Weisberg S. 2019. *An R Companion to Applied Regression*. Thousands Oaks, CA: Sage.

Fuchslueger L., Bahn M., Hasibeder R., Kienzl S., Fritz K., Schmitt M., Watzka M., and Richter A. 2016. Drought history affects grassland plant and microbial carbon turnover during and after a subsequent drought event. J. Ecol. 104: 1453–1465.

Furze J.R., Martin A.R., Nasielski J., Thevathasan N. V., Gordon A.M., and Isaac M.E. 2017. Resistance and resilience of root fungal communities to water limitation in a temperate agroecosystem. Ecol. Evol. 7: 3443–3454.

Gao Y., and Lynch J.P. 2016. Reduced crown root number improves water acquisition under water deficit stress in maize (Zea mays L.). J. Exp. Bot. 67: 4545–4557.

Gardes M., and Bruns T.D. 1993. ITS primers with enhanced specificity for basidiomycetes - application to the identification of mycorrhizae and rusts. Mol. Ecol. 2: 113–118.

Gloor G.B., Macklaim J.M., Pawlowsky-Glahn V., and Egozcue J.J. 2017. Microbiome Datasets Are Compositional: And This Is Not Optional. Front. Microbiol. 8: 1–6.

Griffin D.M. 1985. *A comparison of the roles of bacteria and fungi* (ER Leadbetter and JS Poindexter, Eds.). Boston, MA: Springer US.

Harris R.F. 1981. Effect of Water Potential on Microbial Growth and Activity In: Parr JF, Gardner WR, Elliott LF, eds. *Water Potential Relations in Soil Microbiology*. Madison W.I.: Soil

Science Society of America, 23–95.

Harrison X.A., Donaldson L., Correa-Cano M.E., Evans J., Fisher D.N., Goodwin C.E.D., Robinson B.S., Hodgson D.J., and Inger R. 2018. A brief introduction to mixed effects modelling and multi-model inference in ecology. PeerJ 6: e4794.

Hassan K., Carrillo Y., and Nielsen U.N. 2021. The effect of prolonged drought legacies on plant–soil feedbacks (F Pugnaire, Ed.). J. Veg. Sci. 32: 1–17.

Hawkes C. V., and Keitt T.H. 2015. Resilience vs. historical contingency in microbial responses to environmental change. Ecol. Lett. 18: 612–625.

Hawkes C. V., Kivlin S.N., Rocca J.D., Huguet V., Thomsen M.A., and Suttle K.B. 2011. Fungal community responses to precipitation. Glob. Chang. Biol. 17: 1637–1645.

Henry A., Doucette W., Norton J., and Bugbee B. 2007. Changes in Crested Wheatgrass Root Exudation Caused by Flood, Drought, and Nutrient Stress. J. Environ. Qual. 36: 904–912.

Hooper D.U., Chapin F.S., Ewel J.J., Hector A., Inchausti P., Lavorel S., Lawton J.H., Lodge D.M., Loreau M., Naeem S., Schmid B., Setälä H., Symstad A.J., Vandermeer J., and Wardle D.A. 2005. Effects of biodiversity on ecosystem functioning: A consensus of current knowledge. Ecol. Monogr. 75: 3–35.

Huang K., Sun X., Zou Y., Li Huihe, Xu P., Zhang W., Zhang Y., Li Honglei, Sun H., Wang W., Pang M., and Luo J. 2022. Comparison of the Endophytic Bacterial Microbiota of Asymptomatic and Symptomatic Ginger Rhizomes During the Activation of Adventitious Bud Development. Plant Dis. 106: 2470–2479.

Jing J., Cong W.F., and Bezemer T.M. 2022. Legacies at work: plant–soil–microbiome interactions underpinning agricultural sustainability. Trends Plant Sci. 27: 781–792.

Kaisermann A., de Vries F.T., Griffiths R.I., and Bardgett R.D. 2017. Legacy effects of drought on plant–soil feedbacks and plant–plant interactions. New Phytol. 215: 1413–1424.

Karlowsky S., Augusti A., Ingrisch J., Hasibeder R., Lange M., Lavorel S., Bahn M., and Gleixner G. 2018. Land use in mountain grasslands alters drought response and recovery of carbon allocation and plant-microbial interactions. J. Ecol. 106: 1230–1243.

Killham K., and Firestone M.K. 1984. Salt stress control of intracellular solutes in streptomycetes indigenous to saline soils. Appl. Environ. Microbiol. 47: 301–306.

Korell L., Auge H., Chase J.M., Harpole W.S., and Knight T.M. 2021. Responses of plant diversity to precipitation change are strongest at local spatial scales and in drylands. Nat. Commun. 12: 2489.

Kuhn M. 2008. Building Predictive Models in R Using the caret Package. J. Stat. Softw. 28: 159–160.

Kuznetsova A., Brockhoff P.B., and Christensen R.H.B. 2017. lmerTest Package: Tests in Linear Mixed Effects Models. J. Stat. Softw. 82.

Lau J.A., and Lennon J.T. 2012. Rapid responses of soil microorganisms improve plant fitness in novel environments. Proc. Natl. Acad. Sci. 109: 14058–14062.

Lenth R., Love J., and Herve M. 2020. emmeans: Estimated Marginal Means, aka Least-Squares Means. https://cran.r-project.org/package=emmeans.

De Long J.R., Semchenko M., Pritchard W.J., Cordero I., Fry E.L., Jackson B.G., Kurnosova K., Ostle N.J., Johnson D., Baggs E.M., and Bardgett R.D. 2019. Drought soil legacy overrides maternal effects on plant growth. Funct. Ecol. 33: 1400–1410.

Lozano Y.M., Aguilar-Trigueros C.A., Ospina J.M., and Rillig M.C. 2022. Drought legacy effects on root morphological traits and plant biomass via soil biota feedback. New Phytol. 236: 222–234.

Lynch J.P., Chimungu J.G., and Brown K.M. 2014. Root anatomical phenes associated with water acquisition from drying soil: Targets for crop improvement. J. Exp. Bot. 65: 6155–6166.

Manzoni S., Schimel J.P., and Porporato A. 2012. Responses of soil microbial communities to water stress: results from a meta-analysis. Ecology 93: 930–938.

Martin M. 2011. Cutadapt removes adapter sequences from high-throughput sequencing reads. EMBnet.journal 17: 10.

McMurdie P.J., and Holmes S. 2013. phyloseq: An R Package for Reproducible Interactive Analysis and Graphics of Microbiome Census Data. PLoS One 8: e61217.

Minervini F., Celano G., Lattanzi A., Tedone L., De Mastro G., Gobbetti M., and De Angelis M. 2015. Lactic Acid Bacteria in Durum Wheat Flour Are Endophytic Components of the Plant during Its Entire Life Cycle. Appl. Environ. Microbiol. 81: 6736–6748.

Naylor D., and Coleman-Derr D. 2018. Drought Stress and Root-Associated Bacterial Communities. Front. Plant Sci. 8: 1–16.

Naylor D., DeGraaf S., Purdom E., and Coleman-Derr D. 2017. Drought and host selection influence bacterial community dynamics in the grass root microbiome. ISME J. 11: 2691–2704.

Neilson J.W., Califf K., Cardona C., Copeland A., van Treuren W., Josephson K.L., Knight R., Gilbert J.A., Quade J., Caporaso J.G., and Maier R.M. 2017. Significant Impacts of Increasing Aridity on the Arid Soil Microbiome. mSystems 2.

Oksanen J., Guillaume Blanchet F., Friendly M., Kindt R., Legendre P., McGlinn D., Minchin P.R., O'Hara R.B., Simpson G.L., Solymos P., Stevens M.H.H., Szoecs E., and Wagner H. 2019. vegan: Community Ecology Package.

Panke-Buisse K., Poole A.C., Goodrich J.K., Ley R.E., and Kao-Kniffin J. 2015. Selection on

soil microbiomes reveals reproducible impacts on plant function. ISME J. 9: 980–989.

Parada A.E., Needham D.M., and Fuhrman J.A. 2016. Every base matters: assessing small subunit rRNA primers for marine microbiomes with mock communities, time series and global field samples. Environ. Microbiol. 18: 1403–1414.

Peralta A.L., Sun Y., McDaniel M.D., and Lennon J.T. 2018. Crop rotational diversity increases disease suppressive capacity of soil microbiomes. Ecosphere 9.

Preece C., and Peñuelas J. 2016. Rhizodeposition under drought and consequences for soil communities and ecosystem resilience. Plant Soil 409: 1–17.

Putten W.H., Bradford M.A., Pernilla Brinkman E., Voorde T.F.J., and Veen G.F. 2016. Where, when and how plant–soil feedback matters in a changing world. Funct. Ecol. 30: 1109–1121.

R Core Team. 2021. R: A Language and Environment for Statistical Computing.

Raaijmakers J.M., Paulitz T.C., Steinberg C., Alabouvette C., and Moënne-Loccoz Y. 2009. The rhizosphere: a playground and battlefield for soilborne pathogens and beneficial microorganisms. Plant Soil 321: 341–361.

Santos-Medellín C., Edwards J., Liechty Z., Nguyen B., and Sundaresan V. 2017. Drought Stress Results in a Compartment-Specific Restructuring of the Rice Root-Associated Microbiomes. MBio 8: 1–15.

Schimel J., Balser T.C., and Wallenstein M. 2007. Microbial stress-response physiology and its implications for ecosystem function. Ecology 88: 1386–1394.

Schimel J.P., Scott W.J., and Killham K. 1989. Changes in Cytoplasmic Carbon and Nitrogen Pools in a Soil Bacterium and a Fungus in Response to Salt Stress. Appl. Environ. Microbiol. 55: 1635–1637.

Schultz C.R., Brantley K.M., and Wallace J.G. 2022. The role of genetic variation in Zea mays response to beneficial endophytes. Plant Growth Regul. 98: 167–177.

Sebastian J., Yee M.-C., Goudinho Viana W., Rellán-Álvarez R., Feldman M., Priest H.D., Trontin C., Lee T., Jiang H., Baxter I., Mockler T.C., Hochholdinger F., Brutnell T.P., and Dinneny J.R. 2016. Grasses suppress shoot-borne roots to conserve water during drought. Proc. Natl. Acad. Sci. 113: 8861–8866.

Sharp R.E., and Davies W.J. 1979. Solute regulation and growth by roots and shoots of water-stressed maize plants. Planta 147: 43–49.

Stafford W.H.L., Baker G.C., Brown S.A., Burton S.G., and Cowan D.A. 2005. Bacterial diversity in the rhizosphere of Proteaceae species. Environ. Microbiol. 7: 1755–1768.

Strom N., Hu W., Haarith D., Chen S., and Bushley K. 2020. Interactions between soil properties, fungal communities, the soybean cyst nematode, and crop yield under continuous

corn and soybean monoculture. Appl. Soil Ecol. 147: 103388.

Sumner D.R., Gascho G.J., Johnson A.W., Hook J.E., and Threadgill E.D. 1990. Root Diseases, Populations of Soil Fungi, and Yield Decline in Continuous Double-Crop Corn. Plant Dis. 74: 704.

Svenningsson H., Sundin P., and Liljenberg C. 1990. Lipids, carbohydrates and amino acids exuded from the axenic roots of rape seedlings exposed to water-deficit stress. Plant, Cell Environ. 13: 155–162.

UNITE Community. 2017. UNITE general FASTA release.

Veresoglou S.D., Li G.C., Chen J., and Johnson D. 2022. Direction of plant–soil feedback determines plant responses to drought. Glob. Chang. Biol. 28: 3995–3997.

Větrovský T., Kohout P., Kopecký M., *et al.* 2019. A meta-analysis of global fungal distribution reveals climate-driven patterns. Nat. Commun. 10: 1–9.

Vidaver A.K., and Mandel M. 1974. Corynebacterium nebraskense, a New, Orange-Pigmented Phytopathogenic Species. Int. J. Syst. Bacteriol. 24: 482–485.

Vik U., Logares R., Blaalid R., Halvorsen R., Carlsen T., Bakke I., Kolstø A.-B., Økstad O.A., and Kauserud H. 2013. Different bacterial communities in ectomycorrhizae and surrounding soil. Sci. Rep. 3: 3471.

de Vries F.T., Liiri M.E., Bjørnlund L., Bowker M.A., Christensen S., Setälä H.M., and Bardgett R.D. 2012. Land use alters the resistance and resilience of soil food webs to drought. Nat. Clim. Chang. 2: 276–280.

Wachowska U., and Rychcik B. 2023. Plants control the structure of mycorrhizal and pathogenic fungal communities in soil in a 50-year maize monoculture experiment. Plant Soil 484: 133–153.

Wagner M.R., Roberts J.H., Balint-Kurti P., and Holland J.B. 2020. Heterosis of leaf and rhizosphere microbiomes in field-grown maize. New Phytol. 228: 1055–1069.

Wan X., Chen X., Huang Z., and Chen H.Y.H. 2021. Global soil microbial biomass decreases with aridity and land-use intensification. Glob. Ecol. Biogeogr. 30: 1056–1069.

Wang G., Bei S., Li J., Bao X., Zhang Jiudong, Schultz P.A., Li H., Li L., Zhang F., Bever J.D., and Zhang J. 2021. Soil microbial legacy drives crop diversity advantage: Linking ecological plant–soil feedback with agricultural intercropping. J. Appl. Ecol. 58: 496–506.

Wang Q., Garrity G.M., Tiedje J.M., and Cole J.R. 2007. Naïve Bayesian Classifier for Rapid Assignment of rRNA Sequences into the New Bacterial Taxonomy. Appl. Environ. Microbiol. 73: 5261–5267.

Wang X., Shi W., Wang J., Gao Z., Li S., Wang N., and Shi Q. 2021. Control of Southern Root-knot Nematodes on Tomato and Regulation of Soil Bacterial Community by Biofumigation with

Zanthoxylum bungeanum Seed. Hortic. Plant J. 7: 49–58.

White T.J., Burns T., Lee S., and Taylor J. 1990. Amplification and direct sequencing of fungal ribosomal RNA genes for phylogenetics In: *PCR protocols: a guide to methods and applications*. San Diego, CA: Academic Press, 315–322.

Wright M.N., and Ziegler A. 2017. ranger : A Fast Implementation of Random Forests for High Dimensional Data in C++ and R. J. Stat. Softw. 77.

Wyatt T.T., Wösten H.A.B., and Dijksterhuis J. 2013. Fungal Spores for Dispersion in Space and Time In: *Advances in Applied Microbiology*.43–91.

Xu L., and Coleman-Derr D. 2019. Causes and consequences of a conserved bacterial root microbiome response to drought stress. Curr. Opin. Microbiol. 49: 1–6.

Xu L., Dong Z., Chiniquy D., *et al.* 2021. Genome-resolved metagenomics reveals role of iron metabolism in drought-induced rhizosphere microbiome dynamics. Nat. Commun. 12: 3209.

Xu L., Naylor D., Dong Z., *et al.* 2018. Drought delays development of the sorghum root microbiome and enriches for monoderm bacteria. Proc. Natl. Acad. Sci. 115: E4284–E4293.

Yu A.O., Leveau J.H.J., and Marco M.L. 2020. Abundance, diversity and plant-specific adaptations of plant-associated lactic acid bacteria. Environ. Microbiol. Rep. 12: 16–29.

Zarraonaindia I., Owens S.M., Weisenhorn P., West K., Hampton-Marcell J., Lax S., Bokulich N.A., Mills D.A., Martin G., Taghavi S., van der Lelie D., and Gilbert J.A. 2015. The Soil Microbiome Influences Grapevine-Associated Microbiota. MBio 6: e02527-14.

Zhalnina K., Louie K.B., Hao Z., Mansoori N., da Rocha U.N., Shi S., Cho H., Karaoz U., Loqué D., Bowen B.P., Firestone M.K., Northen T.R., and Brodie E.L. 2018. Dynamic root exudate chemistry and microbial substrate preferences drive patterns in rhizosphere microbial community assembly. Nat. Microbiol. 3: 470–480.

Zhan A., Schneider H., and Lynch J.P. 2015. Reduced Lateral Root Branching Density Improves Drought Tolerance in Maize. Plant Physiol. 168: 1603–1615.

Zhang Q., Acuña J.J., Inostroza N.G., Duran P., Mora M.L., Sadowsky M.J., and Jorquera M.A. 2020. Niche Differentiation in the Composition, Predicted Function, and Co-occurrence Networks in Bacterial Communities Associated With Antarctic Vascular Plants. Front. Microbiol. 11: 1–13.

Zhang B.Q., Chen W.D., and Yang X.B. 1998. Occurrence of Pythium species in long-term maize and soybean monoculture and maize/soybean rotation. Mycol. Res. 102: 1450–1452.

Zolla G., Badri D. V., Bakker M.G., Manter D.K., and Vivanco J.M. 2013. Soil microbiomes vary in their ability to confer drought tolerance to Arabidopsis. Appl. Soil Ecol. 68: 1–9.

Supplemental Figures

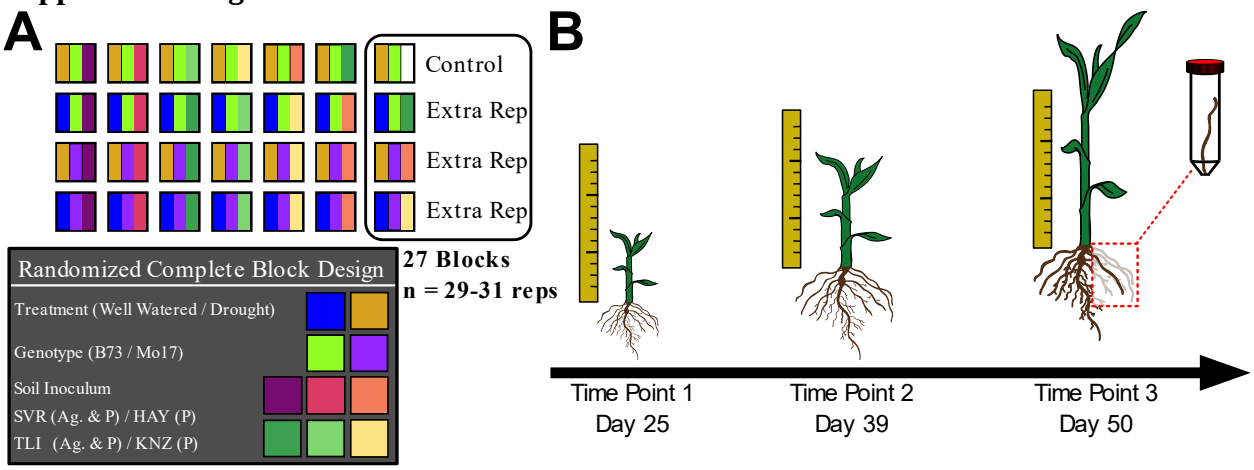

Figure S1. Experimental design. A) A complete randomized block design was used, depicted is a single representative block (number of blocks=27). Each pot was filled with sterile calcined clay soil mix and received a seed of either *Zea mays* genotype B73 or Mo17, was subject to either well-watered or drought conditions, and was inoculated with one of the six inocula. One uninoculated control (denoted with white stripe) and three additional randomized replicates were included per randomized block. **B)** Plant biomass was collected in a time series: for time point one (day 25) and two (day 39), 100 plants each were destructively harvested, then dried for root and shoot biomass. For the third time point (day 50), all remaining plants (n=529 – non-germinates) were harvested. Prior to drying for biomass measures, one nodal root from each plant was collected for amplicon sequencing for bacterial and fungal microbiome composition.

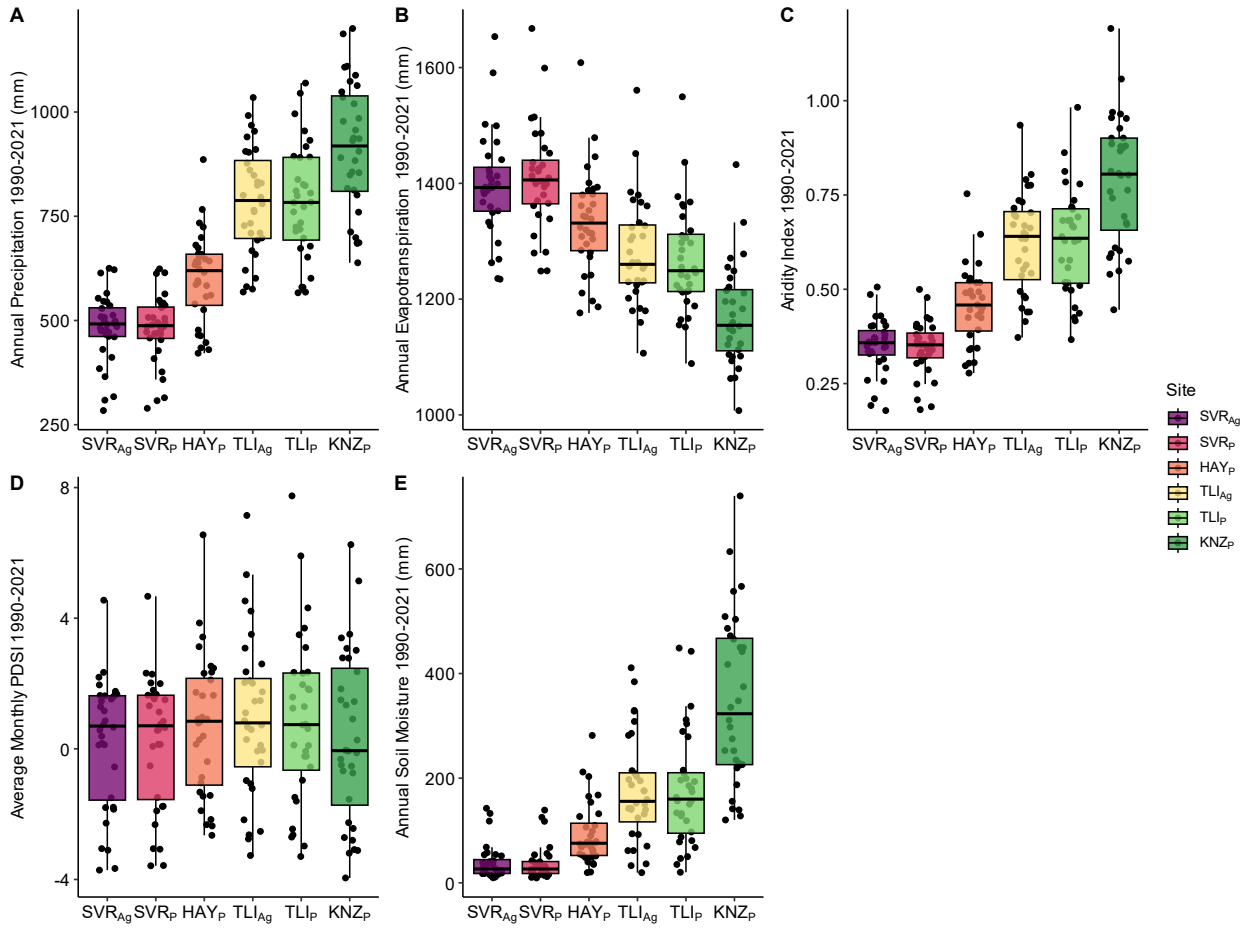

Figure S2. Climatic metrics for each collection site from 1990-2021. A) Annual precipitation, **B)** annual evapotranspiration, **C)** aridity index, **D)** average monthly Palmers Drought Stress Index (PDSI), and **E)** annual soil moisture. Boxplot hinges represent the 1st and 3rd quartiles; whiskers represent 1.5 times the interquartile range.

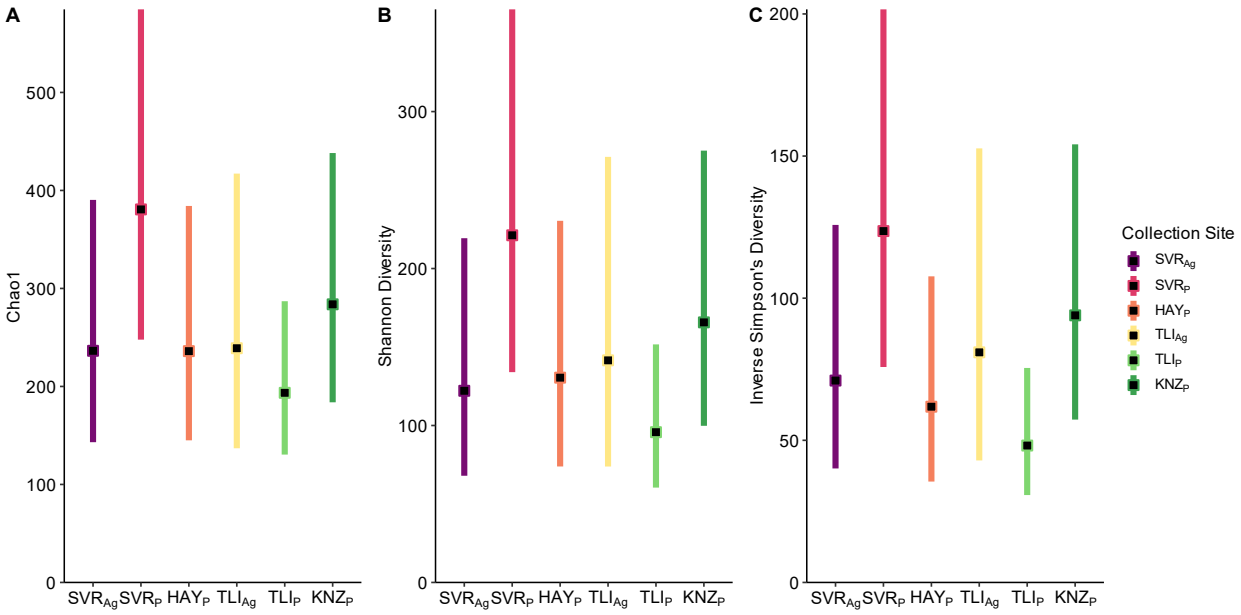

Figure S3. Bacterial alpha diversity values for **A)** Chao1 **B)** Shannon Diversity and **C)** Inverse Simpson's Diversity. Black squares represent estimated marginal means (EMM) for each collection site and colored bars show the 95% confidence intervals for the EMMs.

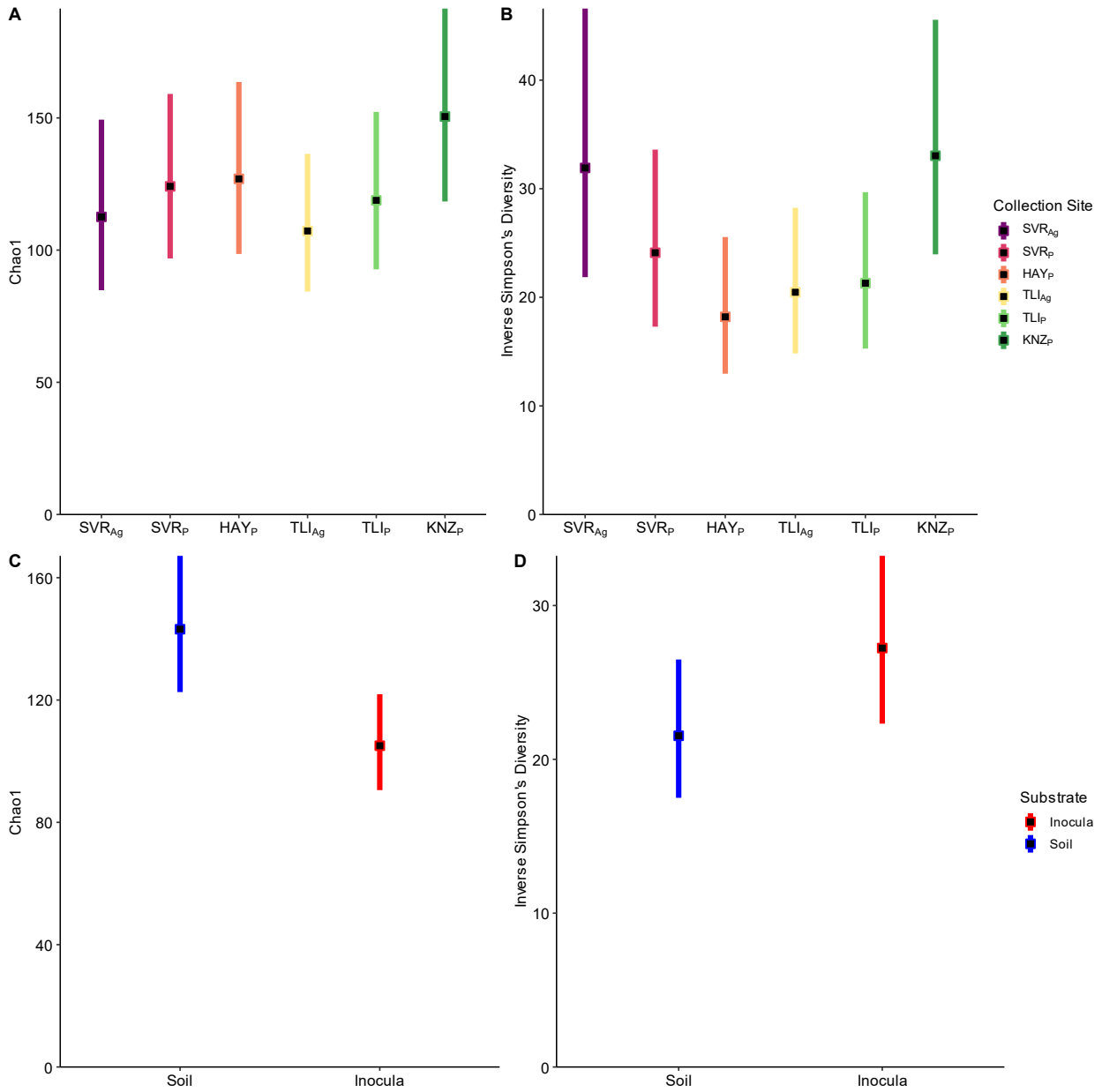

Figure S4. Fungal alpha diversity values for **A/C)** Chao1 and **B/D)** Inverse Simpson's Diversity. Black squares represent estimated marginal means (EMM) for each collection site or substrate and colored bars show the 95% confidence intervals for the EMMs.

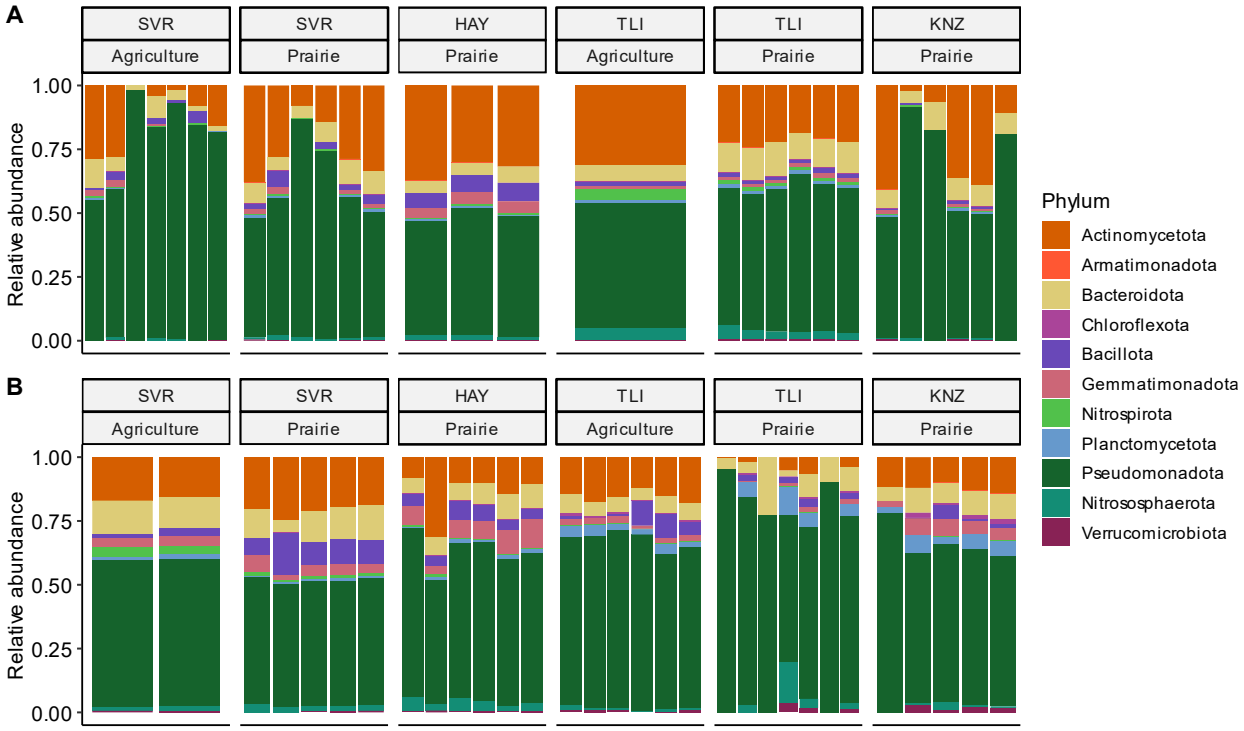

Figure S5. Taxonomic bar plots for bacterial phyla for **A)** soil and **B)** inocula samples. Historical annual precipitation for each collection site (SVR, HAY, TLI, KNZ) increases from left to right. Each sample is represented by a single line with the relative abundance (non CLR transformed data) of each phylum displayed by color.

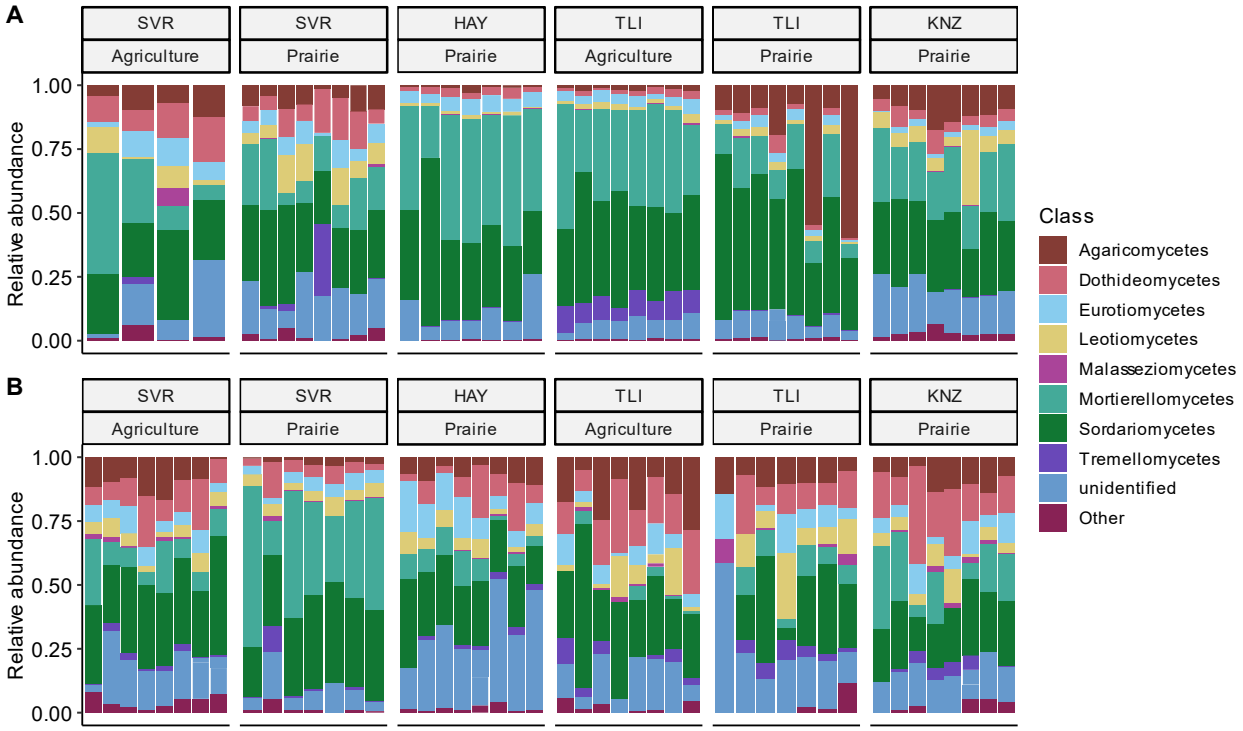

Figure S6. Taxonomic bar plots for fungal classes for **A)** soil and **B)** inocula samples. Historical annual precipitation for each collection site (SVR, HAY, TLI, KNZ) increases from left to right. Each sample is represented by a single line with the relative abundance (non CLR transformed data) of each class displayed by color.

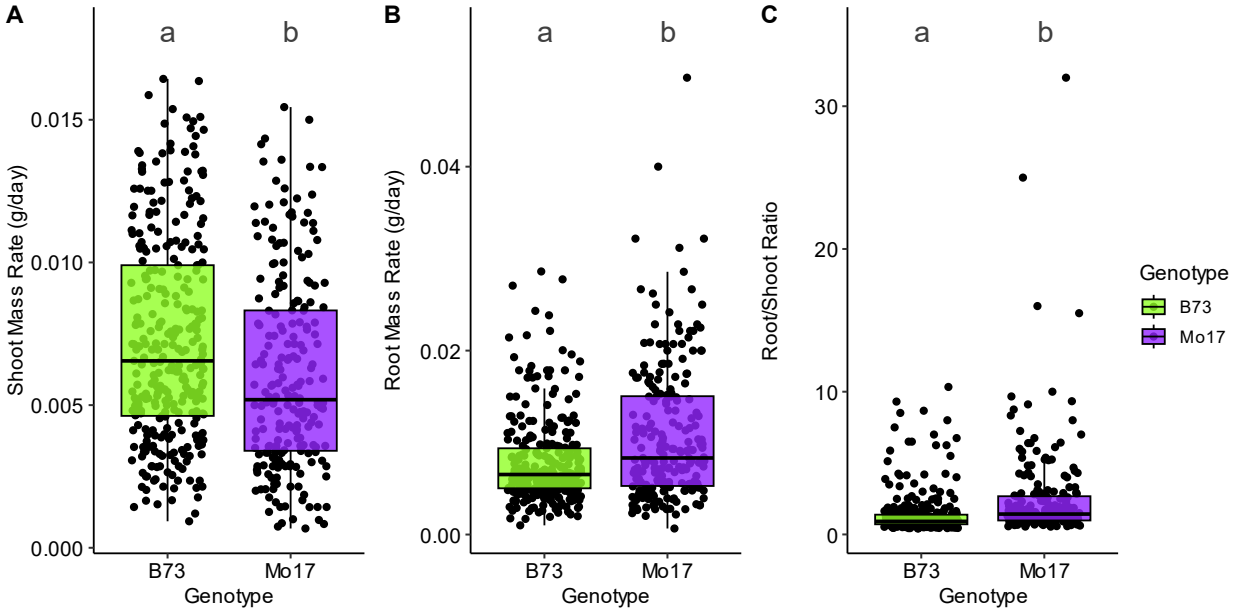

Figure S7. Maize genotypes growth differs across **A)** shoot mass rate, **B)** root mass rate, and **C)** root/shoot ratio. Boxplot hinges represent the 1st and 3rd quartiles; whiskers represent 1.5 times the interquartile range; letters above box plots denote significant differences in estimated marginal means (*p*-value=<0.01; see Table 1 for full ANOVA table).

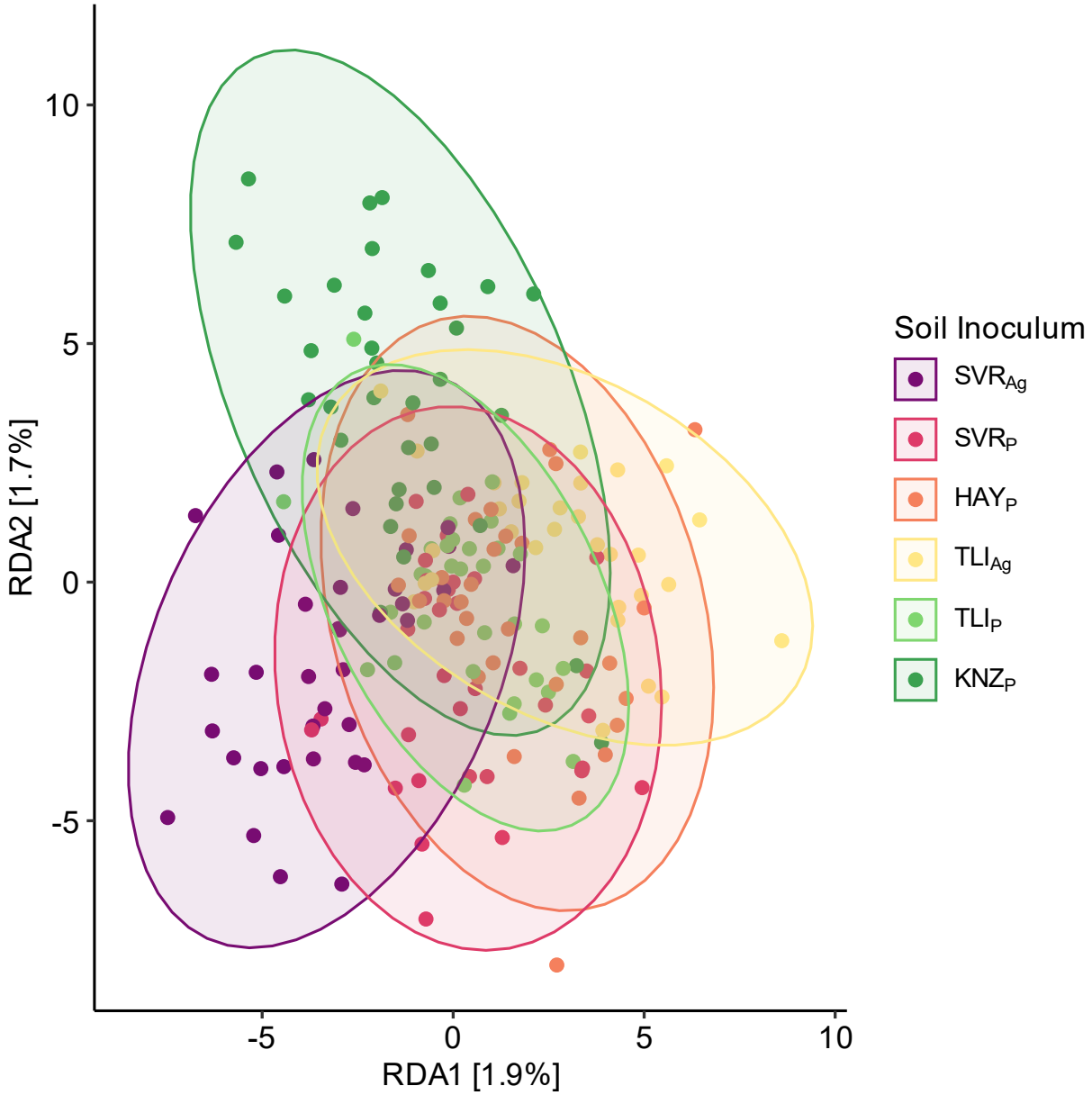

Figure S8. Redundancy analysis for root bacterial community composition. Points are colored by soil inoculum. Normal data ellipses are colored by soil inoculum assuming a multivariate normal distribution.

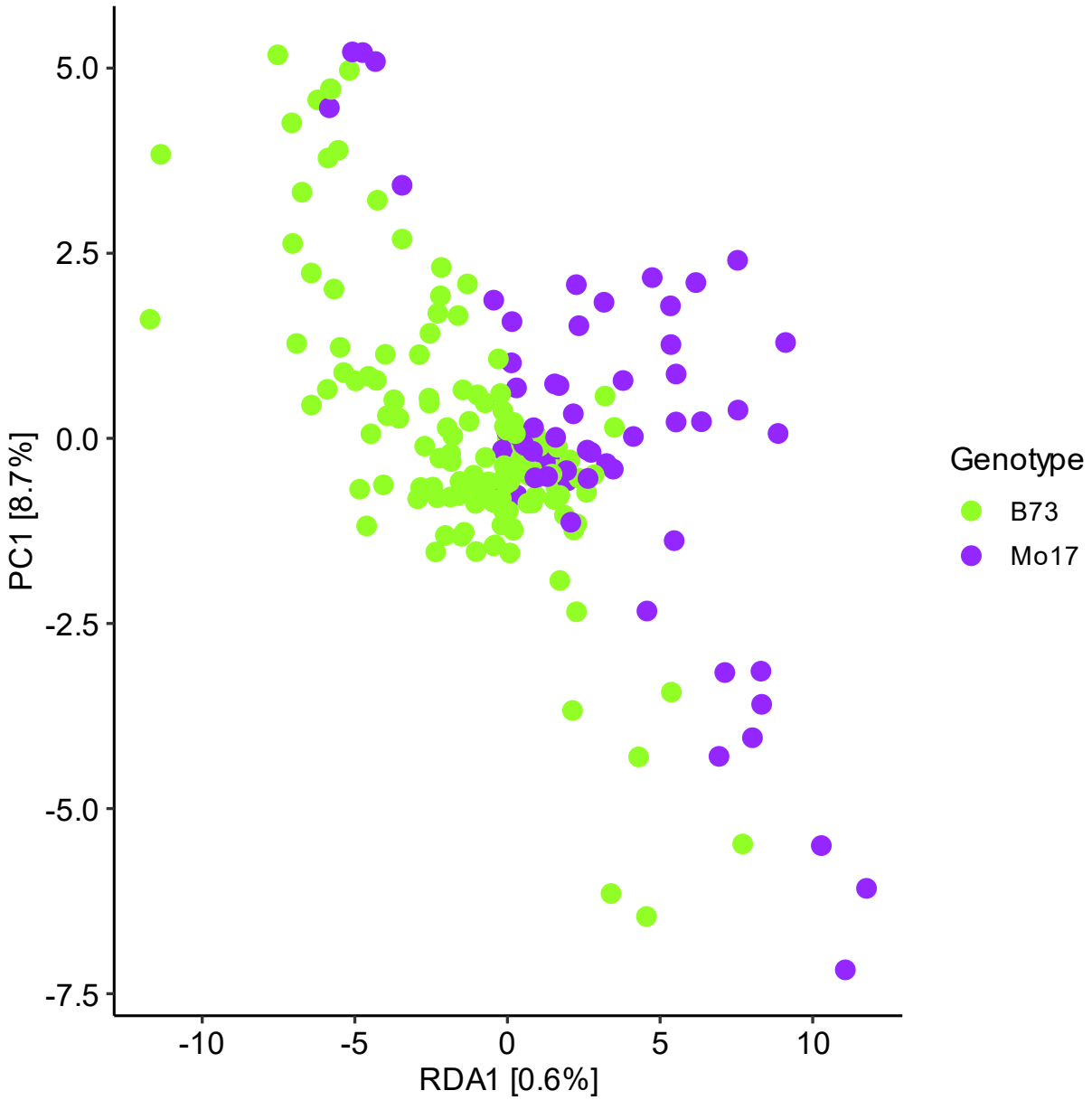

Figure S9. Redundancy analysis for root bacterial community composition. Points are colored by maize genotype.

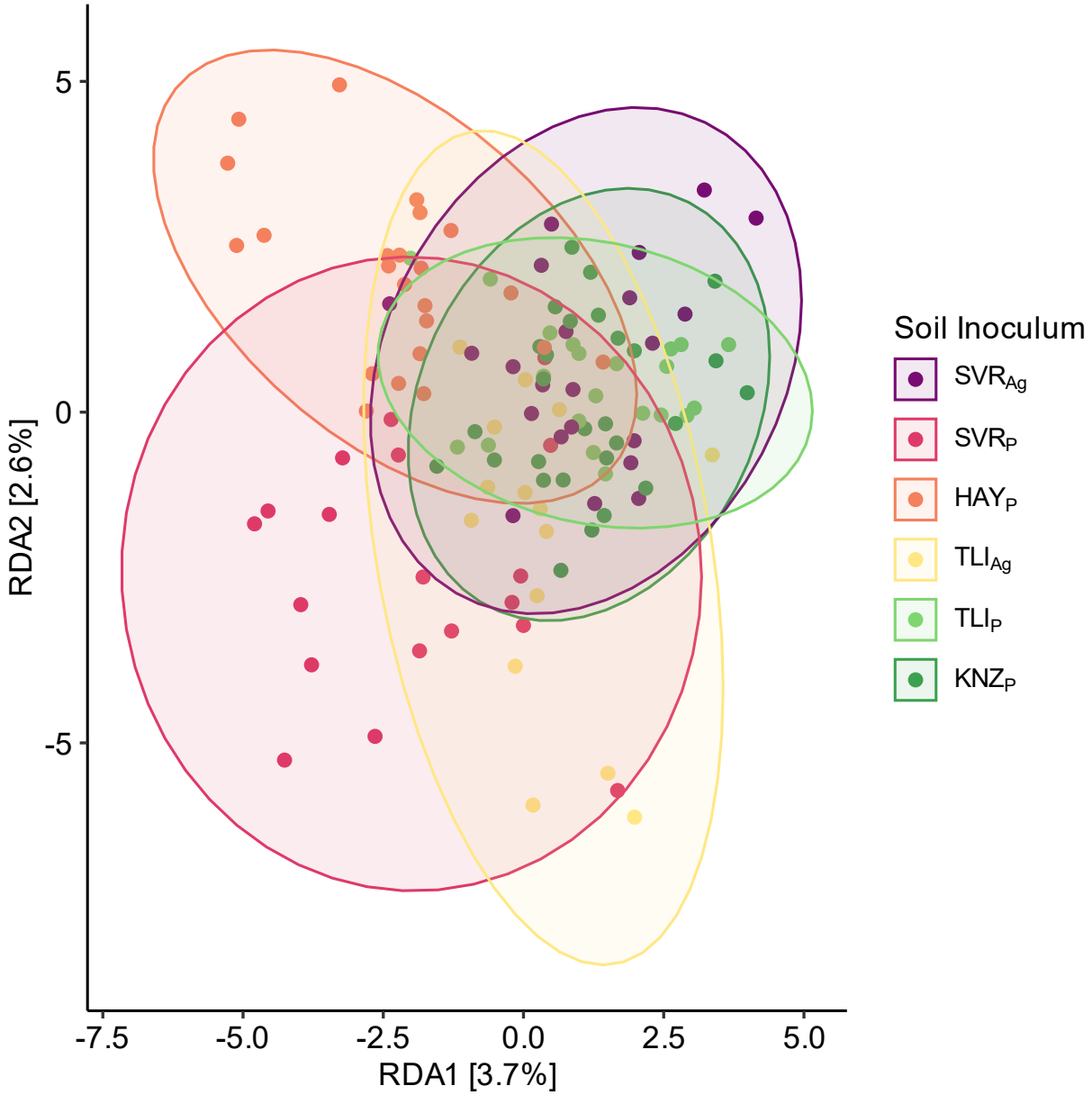

Figure S10. Redundancy analysis for root fungal community composition. Points are colored by soil inoculum. Normal data ellipses are colored by soil inoculum assuming a multivariate normal distribution.

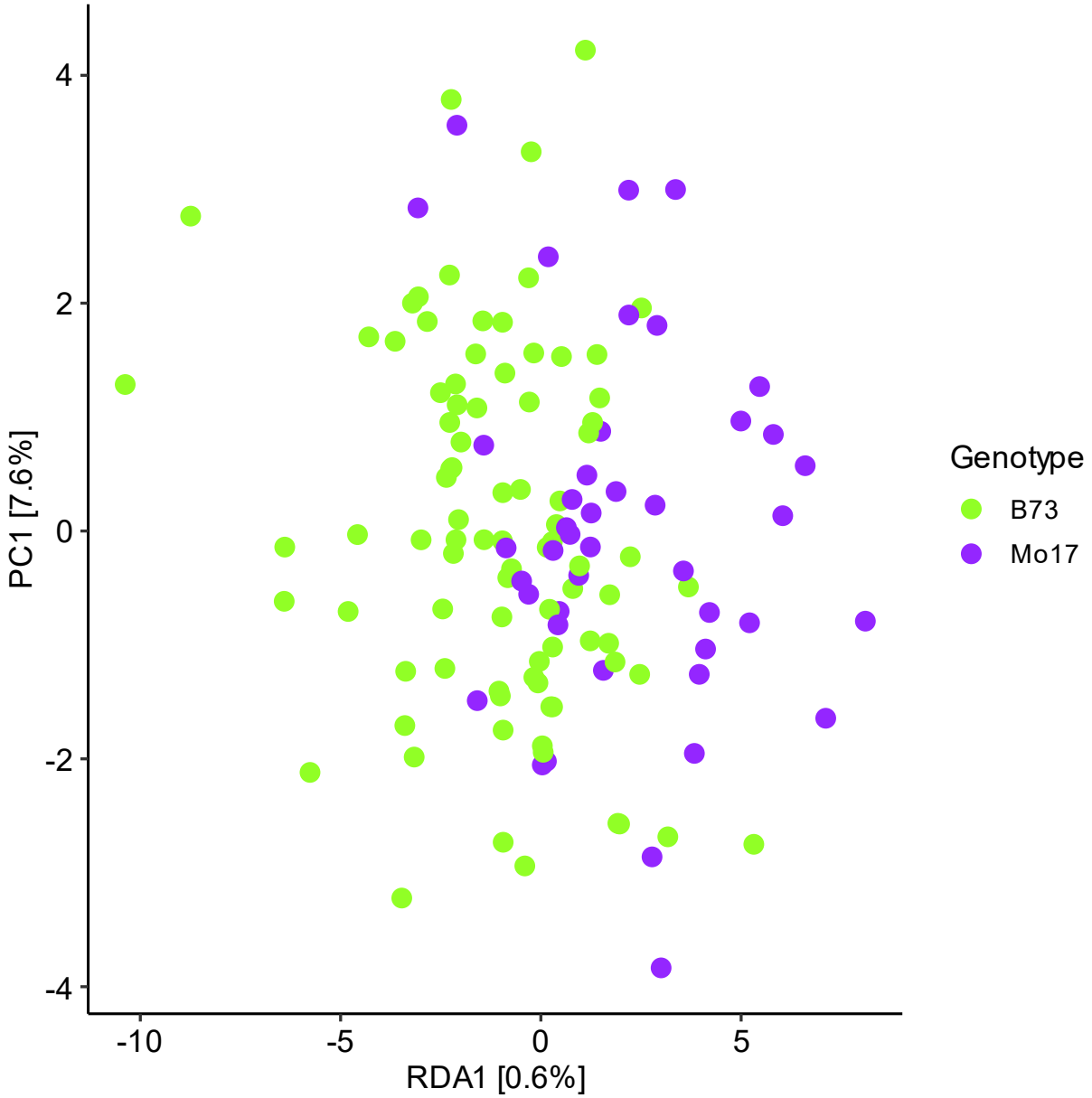

Figure S11. Redundancy analysis for fungal community composition. Points are colored by maize genotype.

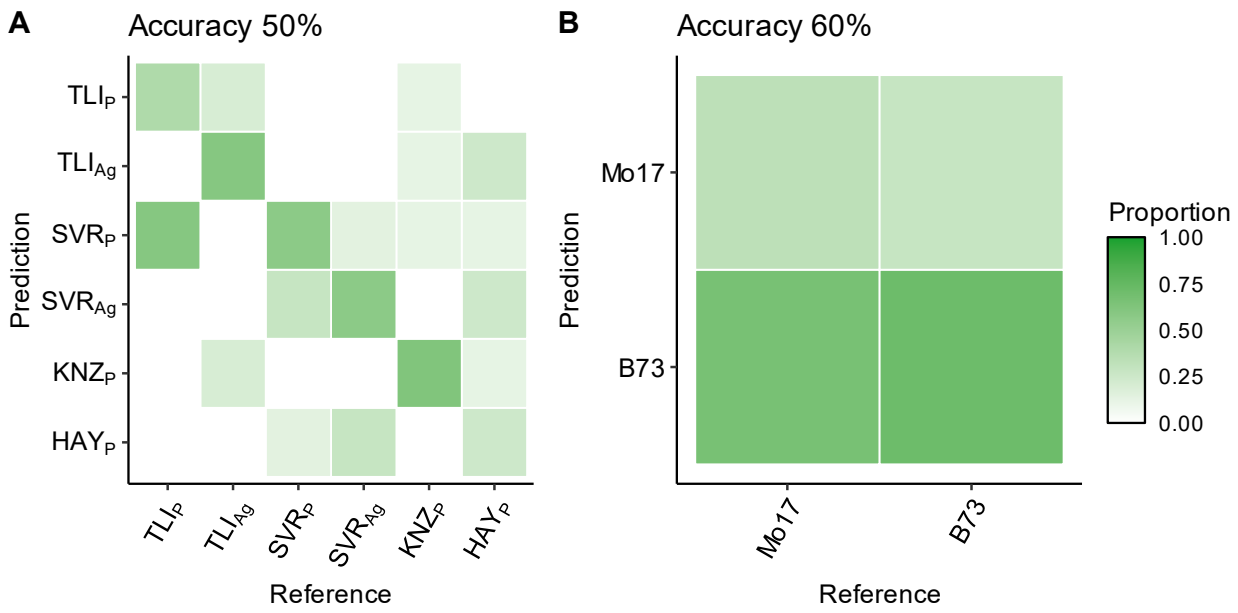

Figure S12. Confusion matrices depicting the classification accuracy of random forest classifiers trained on bacterial data predicting **A)** Soil Inoculum and **B)** Genotype. The models were trained using an 80:20 data split (80% train, 20% test) with 10-fold cross validation, shading represents the proportion of predictions for a label. Labels on the left represent the predicted labels and the labels on the bottom represent the actual labels. The model wide accuracy is given above each confusion matrix, class-wise statistics are provided in table in Table S8.

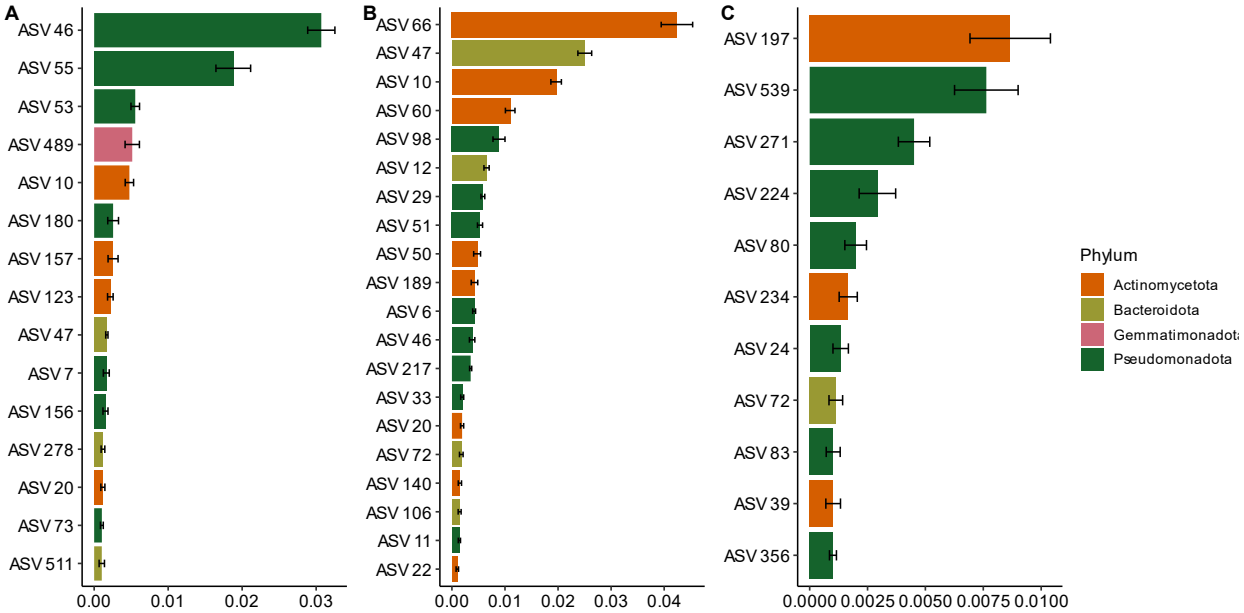

Figure S13. Bacterial ASV importance plots per random forest classifier. Results for **A)** Drought Treatment, **B)** Soil Inoculum, and **C)** Genotype classifiers. For each random forest classifier, 10-fold cross validation was used to assess the mean decrease in accuracy of the classifier when a particular ASV is withheld. Error bars represent the standard error across the 10-folds. Only ASVs with a mean decrease in accuracy greater than 0.001 are shown.

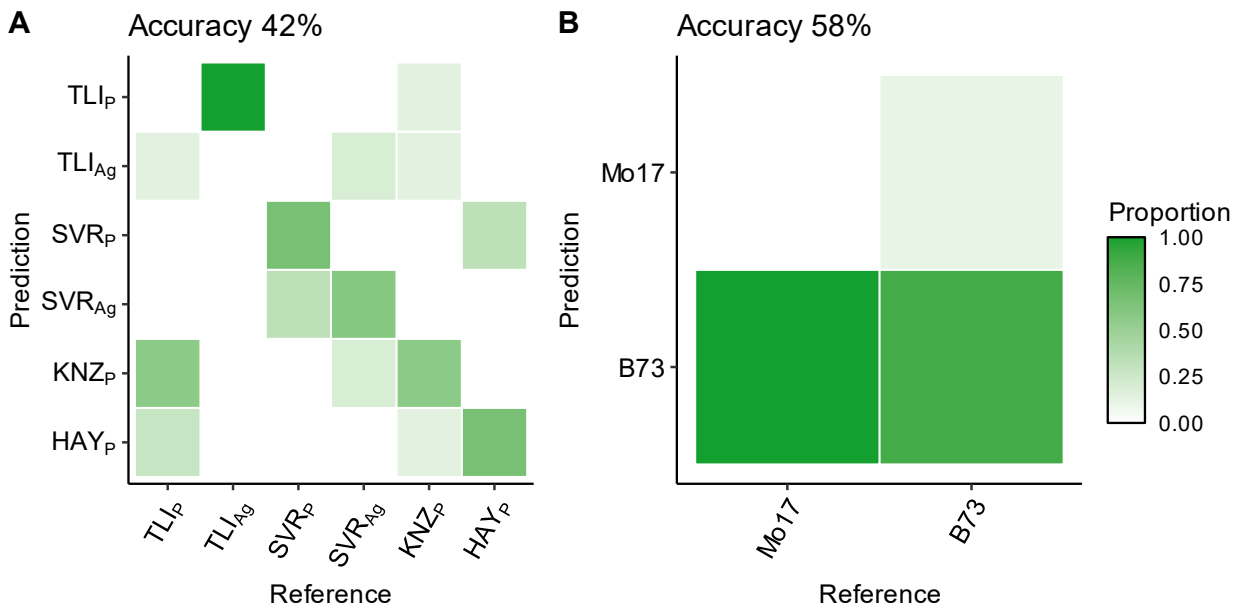

Figure S14. Confusion matrices depicting the classification accuracy of random forest classifiers trained on fungal data predicting **A)** Soil Inoculum and **B)** Genotype. The models were trained using an 80:20 data split (80% train, 20% test) with 10-fold cross validation, shading represents the proportion of predictions for a label. Labels on the left represent the predicted labels and the labels on the bottom represent the actual labels. The model wide accuracy is given above each confusion matrix, class-wise statistics are provided in table in Table S9.

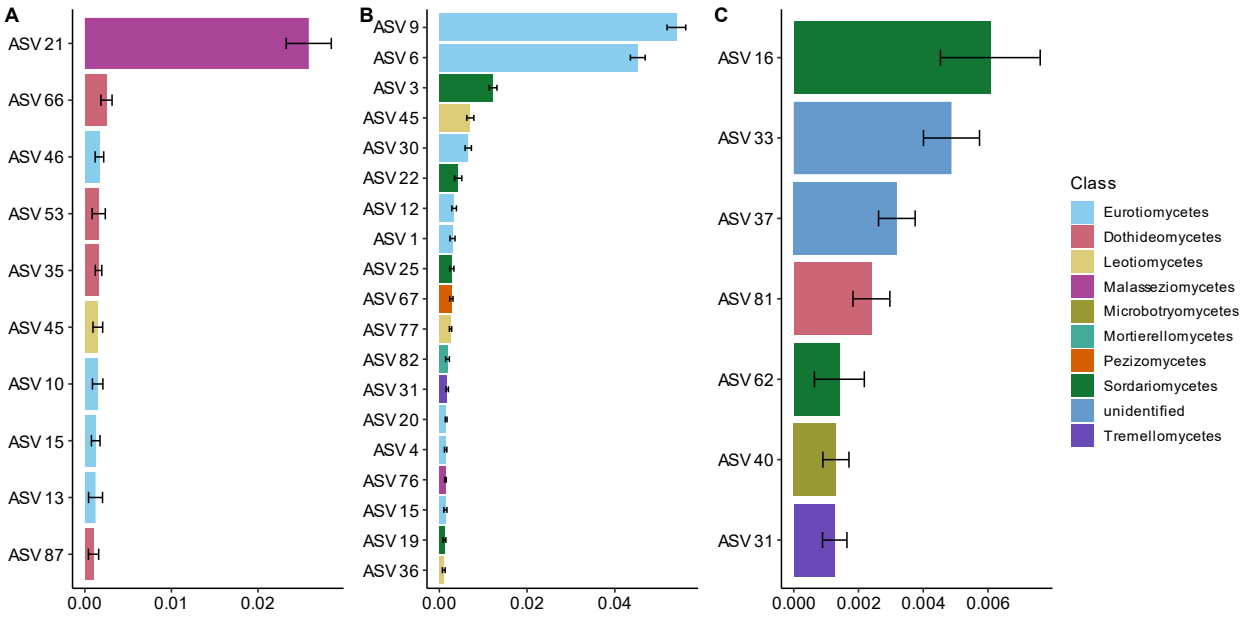

Figure S15. Fungal ASV importance plots per random forest classifier. Results for **A)** Drought Treatment, **B)** Soil Inoculum, and **C)** Genotype classifiers. For each random forest classifier, 10-fold cross validation was used to assess the mean decrease in accuracy of the classifier when a particular ASV is withheld. Error bars represent the standard error across the 10-folds. Only ASVs with a mean decrease in accuracy greater than 0.001 are shown.

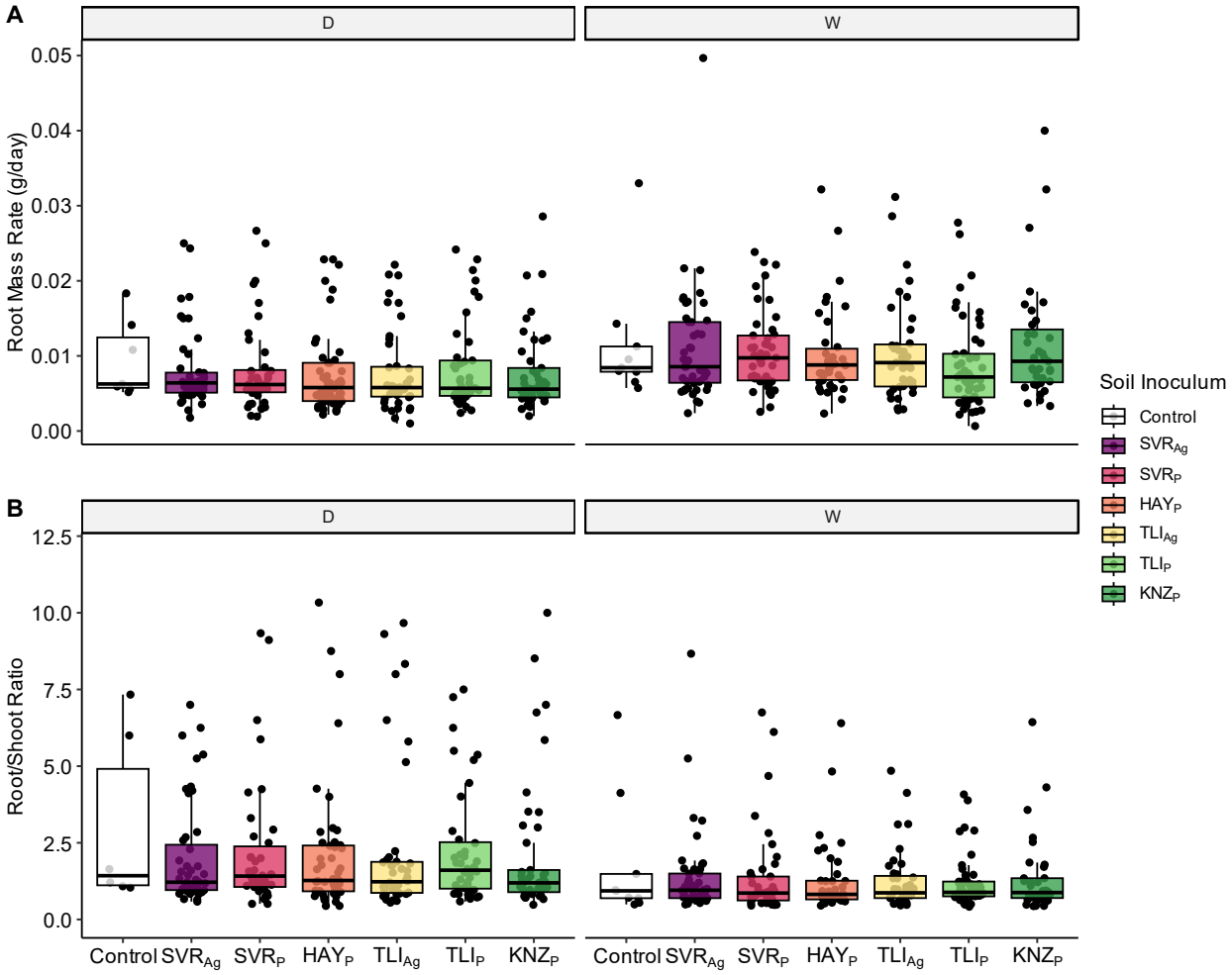

Figure S16. Root growth responses by soil inoculum. Boxplots are colored by soil inoculum for **A)** root mass rate and **B)** root/shoot ratio (four R/S data points were removed to reduce the y axis range and aid in visualization). Separate facets represent drought (D) and well-watered plants (W). Boxplot hinges represent the 1st and 3rd quartiles; whiskers represent 1.5 times the interquartile range.

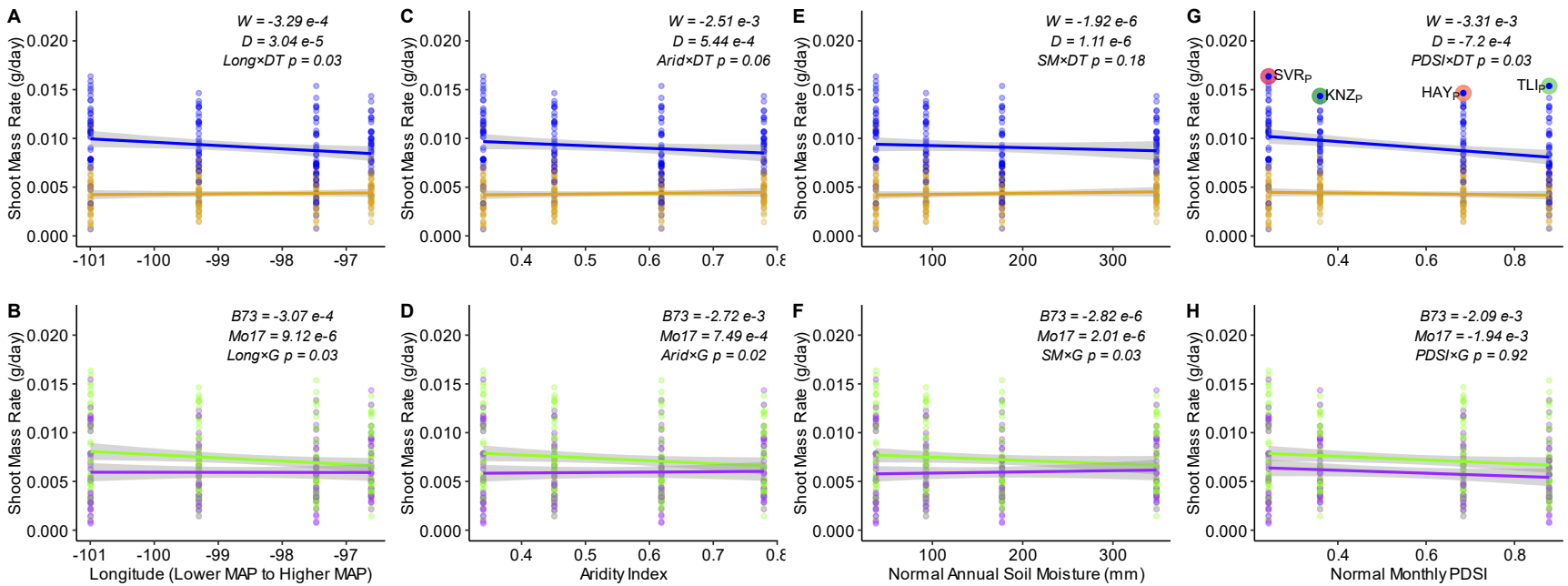

Figure S17. Shoot growth response across longitude and climatic metrics. Trend lines for shoot mass accumulation rate against **A-B)** longitude, **C-D)** Aridity Index, **E-F)** Soil Moisture, and **G-H)** Monthly Palmers Drought Stress Index (PDSI), for interactions with drought treatment and genotype, respectively, for plants inoculated with prairie soils. For PDSI, colors represent the prairie sites as PDSI values do not follow an east to west linear relationship (see Figure S2). For each regression line, grey shading represents the 95% confidence interval.

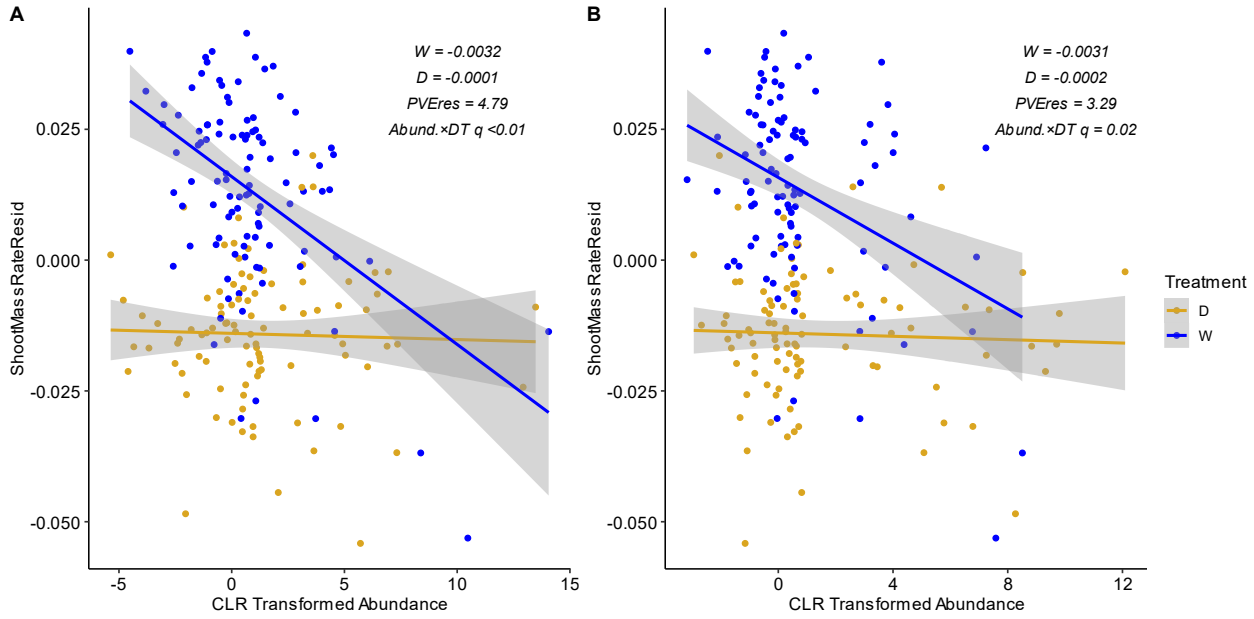

Figure S18. Bacterial families **A)** Corynebacteriaceae and **B)** Streptococcaceae show a significant interaction between CLR transformed abundance and drought treatment for shoot mass rate. For each regression line, grey shading represents the 95% confidence interval.

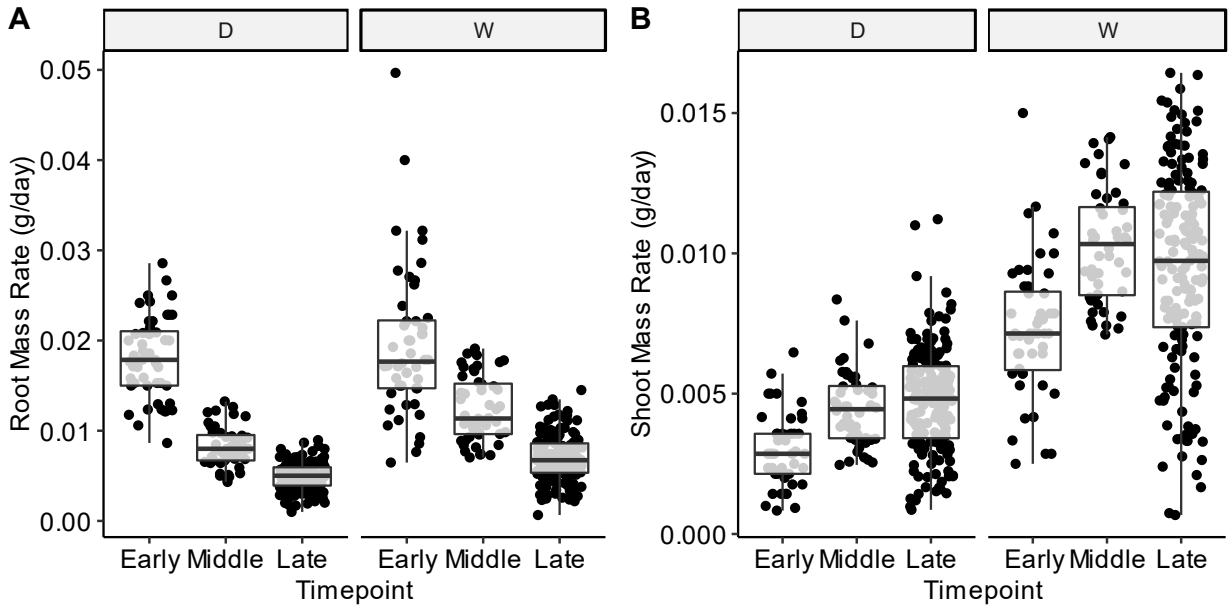

Figure S19. Plant growth rates across the collection time points of the study. A) Root mass rate tended to decrease over the course of the experiment and was modulated by the drought treatment (ANOVA; *'Timepoint × Treatment'* p-value< 0.01). **B**) Shoot mass rate tended to increase over the course of the experiment (ANOVA; *'Timepoint'* p-value< 0.01). Boxplot hinges represent the 1st and 3rd quartiles; whiskers represent 1.5 times the interquartile ran

Supplemental Tables

Table S1. ANOVA table for bacterial alpha diversity metrics of soil samples collected from six locations across the Kansas precipitation gradient.

		log(Chao1)			**log(Shannon's Diversity)**			**log(Inverse Simpson Diversity)**		
Factor	DF	SS	*F*-value	*p*-value	SS	*F*-value	*p*-value	SS	*F*-value	*p*-value
Substrate	1	0.57	1.14	0.29	0.08	0.11	0.74	0.01	0.01	0.92
Collection Site	5	15.9	6.37	**<0.01**	14.41	4.24	**<0.01**	10.67	3.29	**0.01**
Sequence Depth	1	81.02	162.34	**<0.01**	58.20	85.58	**<0.01**	36.96	57.06	**<0.01**
Residual	52	25.95			35.36			33.68		

Bold values denote significant effects, *p*-value<0.05

Table S2. ANOVA table for fungal alpha diversity metrics of soil samples collected from six locations across the Kansas precipitation gradient.

		log(Chao1)			**log(Shannon's Diversity)**			**log(Inverse Simpson Diversity)**		
Factor	DF	SS	*F*-value	*p*-value	SS	*F*-value	*p*-value	SS	*F*-value	*p*-value
Substrate	1	10.50	45.07	**<0.01**	0.02	0.08	0.78	2.99	7.16	**0.01**
Collection Site	5	3.07	2.64	**0.03**	2.67	1.75	0.13	5.21	2.5	**0.04**
Sequence Depth	1	14.67	62.99	**<0.01**	0.45	1.47	0.23	1.28	3.07	0.08
Residual	81	18.87			24.69			33.79		

Bold values denote significant effects, *p*-value<0.05

Table S3. PERMANOVA table for bacterial and fungal community composition of soil and inocula samples collected from six locations across the Kansas precipitation gradient.

	Bacteria					**Fungi**				
Factor	DF	SS	R^2	*F-value*	*p-value*	DF	SS	R^2	*F-value*	*p-value*
Substrate	1	44584	0.10	7.93	**<0.01**	1	32134	0.07	8.05	**<0.01**
Collection Site	5	101664	0.23	3.62	**<0.01**	5	101753	0.22	5.1	**<0.01**
Residual	53	297985	0.67			82	327269	0.71		

Bold values denote significant effects, *p*-value<0.05

Table S4. ANOVA table for maize emergence rate.

	DF	**ChiSq**	***p*-value**
Intercept	1	1072.80	**<0.01**
Genotype (G)	1	7.28	**0.01**
Soil Inoculum (SI)	5	5.42	0.37
G x SI	5	5.97	0.31

Bold values denote significant effects, *p*-value<0.05

Table S5. ANOVA table for bacterial alpha diversity metrics of maize nodal roots.

		Chao1			log(Shannon's Diversity)			log(Inverse Simpson Diversity)		
Factor	DF	SS	F-value	*p*-value	SS	*F*-value	*p*-value	SS	*F*-value	*p*-value
Genotype (G)	1	38929	2.23	0.14	0.17	0.39	0.53	0.02	0.06	0.80
Soil Inoculum (SI)	5	128720	1.48	0.2	4.11	1.92	0.09	3.46	1.81	0.11
Drought Treatment (DT)	1	110485	6.34	**0.01**	0.01	0.03	0.87	0.17	0.45	0.50
SI x DT	5	57853	0.66	0.65	2.35	1.10	0.36	2.72	1.43	0.22

Bold values denote significant effects, *p*-value<0.05

Table S6. ANOVA table for fungal alpha diversity metrics of maize nodal roots.

		Chao1			log(Shannon's Diversity)			log(Inverse Simpson Diversity)		
Factor	DF	SS	*F*-value	*p*-value	SS	*F*-value	*p*-value	SS	*F*-value	*p*-value
Genotype (G)	1	36.25	0.20	0.66	0.17	0.43	0.51	0.17	0.46	0.50
Soil Inoculum (SI)	5	1221.90	1.33	0.26	1.74	0.89	0.49	1.30	0.72	0.61
Drought Treatment (DT)	1	15.85	0.09	0.77	1.04	2.67	0.11	0.77	2.13	0.15
SI x DT	5	1496.80	1.63	0.16	5.95	3.06	**0.01**	5.21	2.89	**0.02**

Bold values denote significant effects, *p*-value<0.05

Table S7. Optimal hyperparameters for bacterial and fungal machine learning classifiers trained to predict treatment, soil inoculum, and genotype.

	Bacteria		Fungi	
Factor	mtry	Minimum Node Side	mtry	Minimum Node Side
Treatment	559	10	64	10
Soil Inoculum	437	5	46	5
Genotype	559	5	10	1

Table S8. Output statistics for bacterial machine learning models predicting treatment, genotype, and soil inoculum.

Metric	Treatment	Genotype	Soil Inoculum					
			SVR_P	SVR_{Ag}	HAY_P	TLI_P	TLI_{Ag}	KNZ_P
Precision	0.737	0.714	0.400	0.500	0.400	0.500	0.500	0.714
Recall	0.700	0.714	0.571	0.571	0.250	0.400	0.600	0.625
F1	0.718	0.714	0.471	0.533	0.308	0.444	0.546	0.667
Prevalence	0.500	0.700	0.175	0.175	0.200	0.125	0.125	0.200
Balanced Accuracy	0.725	0.524	0.695	0.725	0.578	0.671	0.757	0.781

Table S9. Output statistics for fungal machine learning models predicting treatment, genotype, and soil inoculum.

Metric	Treatment	Genotype	Soil Inoculum					
			SVR_P	SVR_{Ag}	HAY_P	TLI_P	TLI_{Ag}	KNZ_P
Precision	0.500	0.625	0.667	0.750	0.400	0.000	0.000	0.444
Recall	0.462	0.8824	0.667	0.600	0.667	0.000	0.000	0.571
F1	0.480	0.7317	0.667	0.667	0.500	NA	NA	0.500
Prevalence	0.500	0.6538	0.115	0.192	0.115	0.269	0.038	0.269
Balanced Accuracy	0.500	0.4412	0.812	0.776	0.768	0.447	0.440	0.654

Table S10. Bacterial taxa across taxonomic levels associated with square root transformed shoot mass rate.

Rank	Taxon	Trait	Model Term	R	X	PVE_{Res}	Rel. Abund.	*q*
Phylum	Actinobacteria	SMR	Abundance	-2.63E-05	-1.22E-02	3.04	13.17	1.73E-02
Class	Actinobacteria	SMR	Abundance	-2.63E-05	-1.22E-02	3.04	13.17	2.34E-02
Class	Deltaproteobacteria	SMR	Abundance	-2.33E-04	-1.36E-02	2.77	0.11	2.34E-02
Order	Actinomycetales	SMR	Abundance	-2.18E-05	-1.25E-02	2.91	13.14	2.75E-02
Order	Myxococcales	SMR	Abundance	-2.33E-04	-1.36E-02	2.77	0.11	2.75E-02
Order	Sphingomonadales	SMR	Abundance	-1.30E-04	-1.24E-02	5.41	1.19	8.25E-04
Family	Actinomycetaceae	SMR	Abundance	-1.85E-03	-1.47E-02	2.18	0.00	3.74E-02
Family	Alcaligenaceae	SMR	Abundance	1.58E-06	-1.42E-02	3.04	0.05	1.30E-02
Family	Beijerinckiaceae	SMR	Abundance	-8.49E-04	-1.46E-02	2.76	0.00	1.69E-02
Family	Corynebacteriaceae	SMR	Abundance	-1.19E-04	-1.40E-02	6.38	0.01	6.45E-05
Family	Dietziaceae	SMR	Abundance	-6.54E-04	-1.38E-02	4.97	0.00	4.08E-04
Family	Lactobacillaceae	SMR	Abundance	3.92E-04	-1.52E-02	3.60	0.14	4.54E-03
Family	Microbacteriaceae	SMR	Abundance	1.11E-04	-1.51E-02	5.14	1.17	4.26E-04
Family	Micrococcaceae	SMR	Abundance	2.58E-05	-1.48E-02	2.77	8.06	1.69E-02

Family	Nocardiaceae	SMR	Abundance	2.84E-04	-1.43E-02	3.63	0.02	5.02E-03
Family	Rhodospirillaceae	SMR	Abundance	-4.46E-04	-1.19E-02	5.54	0.08	4.08E-04
Family	Sinobacteraceae	SMR	Abundance	1.03E-04	-1.46E-02	2.31	0.05	3.37E-02
Family	Sphingomonadaceae	SMR	Abundance	-1.21E-04	-1.25E-02	5.49	1.18	4.08E-04
Family	Streptococcaceae	SMR	Abundance	-1.61E-04	-1.39E-02	5.52	0.02	3.19E-04
Genus	*Amycolatopsis*	SMR	Abundance	-5.16E-05	-1.40E-02	2.96	0.19	2.15E-02
Genus	*Arthrobacter*	SMR	Abundance	1.69E-05	-1.46E-02	2.71	8.20	3.32E-02
Genus	*Chelatococcus*	SMR	Abundance	-8.49E-04	-1.46E-02	2.76	0.00	3.20E-02
Genus	*Corynebacterium*	SMR	Abundance	-1.19E-04	-1.40E-02	6.38	0.01	1.24E-04
Genus	*Cupriavidus*	SMR	Abundance	-3.70E-05	-1.41E-02	4.98	0.02	1.79E-03
Genus	*Dietzia*	SMR	Abundance	-6.54E-04	-1.38E-02	4.97	0.00	1.30E-03
Genus	*Frigoribacterium*	SMR	Abundance	1.42E-03	-1.41E-02	3.63	0.01	9.62E-03
Genus	*Lactobacillus*	SMR	Abundance	3.92E-04	-1.52E-02	3.60	0.14	9.62E-03
Genus	*Minicystis*	SMR	Abundance	1.05E-04	-1.42E-02	2.41	0.00	4.58E-02
Genus	*Rhodococcus*	SMR	Abundance	2.84E-04	-1.43E-02	3.63	0.02	9.62E-03
Genus	*Sphingobium*	SMR	Abundance	-8.99E-05	-1.41E-02	3.64	0.01	9.62E-03
Genus	*Sphingomonas*	SMR	Abundance	-1.47E-04	-1.19E-02	3.19	1.18	1.84E-02
Genus	*Streptococcus*	SMR	Abundance	-1.61E-04	-1.39E-02	5.52	0.02	6.11E-04

Table S11. Fungal taxa across taxonomic levels associated with square root transformed shoot mass rate.

Rank	Taxon	Trait	Model Term	R	X	PVE_{Res}	Rel. Abund.	*q*
Class	Malasseziomycetes	SMR	Abundance	9.97E-05	-1.42E-02	2.92	1.22	3.82E-02
Class	Microbotryomycetes	SMR	Abundance	0.000636	-1.34E-02	4.87	0.66	1.16E-02
Class	Sordariomycetes	SMR	Abundance	2.88E-05	-1.40E-02	4.09	20.65	1.40E-02
Order	Hypocreales	SMR	Abundance	4.75E-05	-1.42E-02	3.28	19.23	4.68E-02
Order	Malasseziales	SMR	Abundance	9.97E-05	-1.42E-02	2.92	1.22	4.86E-02
Order	Sporidiobolales	SMR	Abundance	6.36E-04	-1.34E-02	4.87	0.66	1.47E-02
Family	Hypocreales_fam_Incertae_sedis	SMR	Abundance	6.55E-05	-1.46E-02	4.07	15.23	3.05E-02
Family	Sporidiobolaceae	SMR	Abundance	6.36E-04	-1.34E-02	4.87	0.66	2.63E-02